Table 1
Statistics of data collection and processing.

Values in parentheses are for the highest resolution shell.

	A. suum QFR	*A. suum* QFR with flutolanil
X-ray source	BL44XU (SPring-8)	NW12A (Photon Factory)
Wavelength (Å)	0.900	1.000
Space group	$P2_12_12_1$	$P2_12_12_1$
Unit-cell parameters		
a (Å)	123.75	124.31
b (Å)	129.08	131.63
c (Å)	221.12	222.53
Resolution range (Å)	50.0–2.8 (2.9–2.8)	50.0–3.20 (3.35–3.20)
No. of reflections	587189	207156
Unique reflections	75372	54964
Completeness (%)	89.2 (58.8)	93.9 (84.1)
R_{merge}† (%)	10.5 (36.6)	11.5 (40.0)
$I/\sigma(I)$	8.4 (3.5)	17.4 (1.6)

† $R_{merge} = \sum_{hkl}\sum_i |I_i(hkl) - \langle I(hkl)\rangle| / \sum_{hkl}\sum_i I_i(hkl)$.

of SQR from pig heart mitochondria (Sun *et al.*, 2005; PDB code 1zoy). The sequence identities between the pig and *A. suum* enzymes are 70.4, 68.3, 34.8 and 46.3% for the Fp, Ip, CybL and CybS subunits, respectively. Using X-ray diffraction data in the resolution range 15.0–2.8 Å collected from the flutolanil-free QFR crystal, a promising solution with two molecules per asymmetric unit was obtained and an *R* factor of 0.45 was achieved when the model was subsequently subjected to rigid-body refinement. Starting from the molecular-replacement solution, the structures of the flutolanil-free and flutolanil-bound forms of the *A. suum* QFR are currently being refined and electron density corresponding to bound flutolanil has been identified. The structures of the *A. suum* QFR together with those of the QFRs from *Wolinella succinogenes* (Lancaster *et al.*, 1999) and *Escherichia coli* (Iverson *et al.*, 1999) and the SQRs from *E. coli* (Yankovskaya *et al.*, 2003), pig heart mitochondria (Sun *et al.*, 2005) and avian heart mitochondria (Huang *et al.*, 2006) should help to clarify the structure–function relationships in complex II. In addition, the structure of the *A. suum* QFR complexed with flutolanil should provide information for the structure-based design of anthelminthics.

We are grateful to the staff of BL44XU at SPring-8 and the staff of NW12 and BL-5A at Photon Factory for their help with the collection of X-ray diffraction data. This work was supported in part by a grant from the Japan Aerospace Exploration Agency and by Grants-in-Aid for Scientific Research on Priority Areas from the 21st Century COE Program (F-3), for Creative Scientific Research and Targeted Proteins Research Program from the Japanese Ministry of Education, Culture, Sports, Science and Technology (180 73004, 18GS0314 and 1903610), and for Scientific Research (B) from the Japan Society for the Promotion of Science (18370042). DKI was a research fellow supported by the Japan Society for the Promotion of Science.

References

Collaborative Computational Project, Number 4 (1994). *Acta Cryst.* **D50**, 760–763.
Ernster, L. & Nordenbrand, K. (1967). *Methods Enzymol.* **10**, 86–94.
Huang, L. S., Sun, G., Cobessi, D., Wang, A. C., Shen, J. T., Tung, E. Y., Anderson, V. E. & Berry, E. A. (2006). *J. Biol. Chem.* **281**, 5965–5972.
Inaoka, D. K., Sakamoto, K., Shimizu, H., Shiba, T., Kurisu, G., Nara, T., Aoki, T., Kita, K. & Harada, S. (2008). *Biochemistry*, **47**, 10881–10891.
Ito, Y., Muraguchi, H., Seshime, Y., Oita, S. & Yanagi, S. O. (2004). *Mol. Genet. Genomics*, **272**, 328–335.
Iverson, T. M., Luna-Chaves, C., Cecchini, G. & Rees, D. C. (1999). *Science*, **284**, 1961–1966.
Iwata, F., Shinjyo, N., Amino, H., Sakamoto, K., Islam, M. K., Tsuji, N. & Kita, K. (2008). *Parasitol. Int.* **57**, 54–61.
Jancarik, J. & Kim, S.-H. (1991). *J. Appl. Cryst.* **24**, 409–411.
Kita, K. & Takamiya, S. (2002). *Adv. Parasitol.* **51**, 95–131.
Lancaster, C. R. D., Kröger, A., Auer, M. & Michel, H. (1999). *Nature (London)*, **402**, 377–385.
Matsumoto, J., Sakamoto, K., Shinjyo, N., Kido, Y., Yamamoto, N., Yagi, K., Miyoshi, H., Nonaka, N., Katakura, K., Kita, K. & Oku, Y. (2008). *Antimicrob. Agents. Chemother.* **52**, 164–170.
Matthews, B. W. (1968). *J. Mol. Biol.* **33**, 491–497.
Miyadera, H., Shiomi, K., Ui, H., Yamaguchi, Y., Masuma, R., Tomoda, H., Miyoshi, H., Osanai, A., Kita, K. & Omura, S. (2003). *Proc. Natl Acad. Sci. USA*, **100**, 473–477.
Navaza, J. (1994). *Acta Cryst.* **A50**, 157–163.
Omura, S. *et al.* (2001). *Proc. Natl Acad. Sci. USA*, **98**, 60–62.
Otwinowski, Z. & Minor, W. (1997). *Methods Enzymol.* **276**, 307–326.
Sun, F., Huo, X., Zhai, Y., Wang, A., Xu, J., Su, D., Bartlam, M. & Rao, Z. (2005). *Cell*, **121**, 1043–1057.
Takamiya, S., Furushima, R. & Oya, H. (1984). *Mol. Biochem. Parasitol.* **13**, 121–134.
Tielens, A. G. M., Rotte, C., van Hellemond, J. J. & Martin, W. (2002). *Trends Biochem. Sci.* **27**, 564–572.
Yankovskaya, V., Horsefield, R., Törnroth, S., Luna-Chaves, C., Miyoshi, H., Léger, C., Byrne, B., Cecchini, C. & Iwata, S. (2003). *Science*, **299**, 700–704.

Mitochondrion 9 (2009) 443–453

Contents lists available at ScienceDirect

Mitochondrion

journal homepage: www.elsevier.com/locate/mito

Identification of mitochondrial Complex II subunits SDH3 and SDH4 and ATP synthase subunits *a* and *b* in *Plasmodium* spp.

Tatsushi Mogi *, Kiyoshi Kita *

Department of Biomedical Chemistry, Graduate School of Medicine, The University of Tokyo, Hongo, Bunkyo-ku, Tokyo 113-0033, Japan

ARTICLE INFO

Article history:
Received 5 February 2009
Received in revised form 3 August 2009
Accepted 6 August 2009
Available online 12 August 2009

Keywords:
ATP synthase
Membrane anchor
Mitochondria
Plasmodium
Succinate dehydrogenase

ABSTRACT

While most protist mitochondrial enzymes could be identified in database, the membrane anchor subunits of Complex II and F_oF_1-ATP synthase of malaria parasites are not annotated. Based on the presence of structural fingerprints or proteomics data from other protists, here we present their candidates. In contrast to canonical subunits, *Plasmodium* Complex II anchors have two transmembrane helices and may coordinate heme *b via* Tyr in place of His. Transmembrane helix IV of ATP synthase subunit *a* lacks an essential Arg residue. Membrane anchors of *Plasmodium* Complex II and ATP synthase are divergent from orthologs and promising targets for new chemotherapeutics.

1. Introduction

Energy metabolism in the malaria parasites is quite different from that of mammalian hosts. The erythrocytic stage cells of *Plasmodium falciparum* cause mortality associated with malaria and are considered to rely on the incomplete oxidation of glucose, with the secretion of end products such as lactate and pyruvate (Sherman, 1998). Diversity in parasite metabolism and enzyme structures will facilitate the development of new antimalarials with novel targets and mechanisms against the drug-resistant strains of *Plasmodium* spp. (Hyde, 2005).

The *Plasmodium* mitochondrion of the erythrocytic stage parasites can oxidize NADH, glycerol-3-phosphate, succinate, dihydroorotate, and amino acids (Pro and Glu), but it is essentially acristate and apparently lacks oxidative phosphorylation and a functional tricarboxylic acid (TCA) cycle (Fry and Beesley, 1991; van Dooren et al., 2006). Pyruvate dehydrogenase is targeted to the apicoplast, not to the mitochondrion (Foth et al., 2005), and thus a major carbon flow from the cytoplasm to the mitochondrion of most eukaryotes is disconnected (Fig. 1). Fumarate inhibited the NADH-dependent reduction of cytochrome *c* and stimulated the oxidation of NADH, indicating an NADH–fumarate reductase pathway for the regeneration of NAD (Fry and Beesley, 1991). Recently, Painter et al. (2007) claimed for the erythrocytic stage cells of *P. falciparum* that the mitochondrial respiratory chain is required only for the regeneration of an oxidized form of ubiquinone, which serves as the electron acceptor for type 2 dihydroorotate dehydrogenase, an essential enzyme for pyrimidine biosynthesis. Thus, it is widely accepted that the majority of the erythrocytic stage parasite's ATP demand is met through glycolysis (Carlton et al., 2002).

In the insect vector stages, malaria parasites need to adapt to changes in available carbon sources from glucose in the mammalian blood to amino acids (e.g., Pro, Glu, His, and Ala (Henn et al., 1998)) in the mosquito hemolymph, which contains the disaccharide trehalose as a dominant sugar species. As amino acids are non-fermentable carbon sources, oxidative phosphorylation with the functional TCA cycle must take place in the insect stages. Proteomic profiling studies clearly demonstrated metabolic readjustments from the glycolytic pathway in the asexual stages trophozoites and schizonts to the TCA cycle in the salivary gland sporozoites (Lasonder et al., 2008). Metabolomic studies on the erythrocytic stage *P. falciparum* demonstrated that Gln was metabolized to L-malate *via* two pathways, the reductive carboxylation pathway through citrate yielding acetyl-CoA and the oxidative pathway through succinate yielding ATP and a precursor of heme biosynthesis (δ-aminolevulinic acid) (Olszewski, Rabinowitz, Llinás, personal communication) (Fig. 1). Thus, amino acids acquired from the mosquito hemolymph or the food vacuole of the erythrocytic stage parasites can be metabolized by entering the TCA cycle as 2-oxoglutarate *via* a bifurcated mechanism using

Abbreviations: FRD, fumarate reductase; SDH, succinate dehydrogenase; TCA, tricarboxylic acid; TM, transmembrane helix.

* Corresponding authors. Tel.: +81 3 5841 3526; fax: +81 3 5841 3444.
E-mail addresses: tmogi@m.u-tokyo.ac.jp (T. Mogi), kitak@m.u-tokyo.ac.jp (K. Kita).

1567-7249/$ - see front matter © 2009 Elsevier B.V. and Mitochondria Research Society. All rights reserved.
doi:10.1016/j.mito.2009.08.004

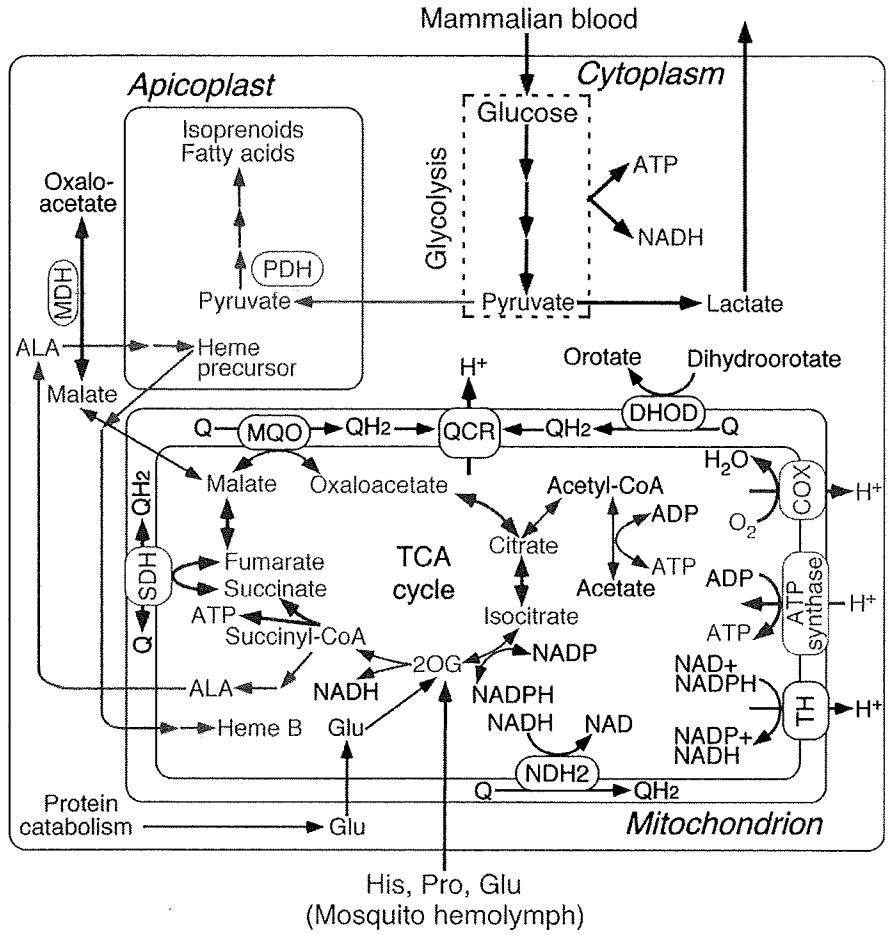

Fig. 1. Metabolic pathway in the human malaria parasite *P. falciparum*. Proton translocation machineries in the mitochondrion are F_oF_1-ATP synthase (ATPase), quinol–cytochrome *c* reductase (QCR), cytochrome *c* oxidase (COX), and NAD(P)-transhydrogenase (TH). Quinone reduction by alternative NADH dehydrogenase (NDH2), succinate dehydrogenase (SDH), malate:quinone oxidoreductase (MQO), and dihydroorotate dehydrogenase (DHOD) do not generate the proton-motive force. NAD-dependent malate dehydrogenase (MDH) and pyruvate dehydrogenase (PDH) are located in the cytoplasm and apicoplast, respectively, and do not participate in TCA cycle. Expression levels of MDH and TCA cycle enzymes (fumarate hydratase, SDH1, succinyl-CoA synthase α subunit, aconitase, and citrate synthase), and α and β subunits of ATP synthase are increased in salivary gland sporozoites while the expression levels of glycolysis pathway enzymes (hexokinase, phosphoglycerate kinase, pyruvate kinase and 6-phosphofructokinase) are increased in asexual blood-stage trophozoites and schizonts [Lasonder et al., 2008; Lasonder, Stunnenberg, personal communication]. A major carbon flow in blood-stage parasites is shown in *red* and possible carbon and energy flow in mosquito stages is shown in *blue*. Pathways absent in *B. bovis* are indicated by *green*. For the clarity, outer membranes of the mitochondrion and apicoplast are not shown. Abbreviations for metabolites are ALA (δ-aminolevulinic acid), DHAP (dihydroxyacetone phosphate), GA3P (glyceraldehyde-3-phosphate), and PEP (phosphoenolpyruvate).

the reductive and oxidative pathways. The resulting NADH and quinols are reoxidized by the respiratory chain, which indirectly drives ATP synthesis by the generation of proton-motive force.

In contrast to *P. falciparum*, the mitochondrion isolated from the erythrocytic stage rodent malaria parasite is cristate and contains more cytochromes (Fry and Beesley, 1991). Succinate respiration, ATP synthesis, and the collapse of the mitochondrial membrane potential by atovaquone (Srivastava et al., 1997), a potent inhibitor of ubiquinol–cytochrome *c* reductase (Complex III), suggest the presence of a functional oxidative phosphorylation system in the erythrocytic rodent parasite mitochondria (Uyemura et al., 2000, 2004). Transcriptome analysis of the erythrocytic human parasites, which have been isolated from infected patients, indicates that canonical mitochondrial functions exist to some extent in the human parasites (Daily et al., 2007). In *Plasmodium* spp., nuclear and mitochondrial genomes encode ubiquinol–cytochrome *c* reductase (QCR, Complex III), cytochrome *c* oxidase (COX, Complex IV), F_oF_1-ATP synthase (Complex V) and all the TCA cycle enzymes including succinate dehydrogenase (SDH, succinate–ubiquinone reductase, Complex II) (Carlton et al., 2002; Gardner et al., 2002). H^+-translocating NADH–ubiquinone reductase (NDH1, Complex I) in the mitochondrial respiratory chain is substituted by alternative NADH dehydrogenase (NDH2, a single-subunit NADH–ubiquinone reductase) (Uyemura et al., 2004; Biagini et al., 2006; Kawahara et al., 2009) (Fig. 1).

It should be noted that the membrane anchor subunits of Complex II (SDH3 (CybL) and SDH4 (CybS)) and of ATP synthase (subunits *a* (ATP6) and *b* (ATP4)) are not annotated in the current database (Carlton et al., 2002; Gardner et al., 2002), even though they are essential for transfer of chemical energy to ubiquinone and proton translocation, respectively (Fig. 2). Accordingly, the complete ATP synthase is assumed to be absent in *Plasmodium* spp. (Carlton et al., 2002; Gardner et al., 2002; Fry et al., 1990; Vaidya and Mather, 2005).

Recently, we characterized characterized Complex II of the erythrocytic stage *Plasmodium yoelii yoelii* mitochondria and found evidence for the presence of SDH3 and SDH4 (Kawahara et al., 2009). Because of the low expression of TCA cycle enzymes in

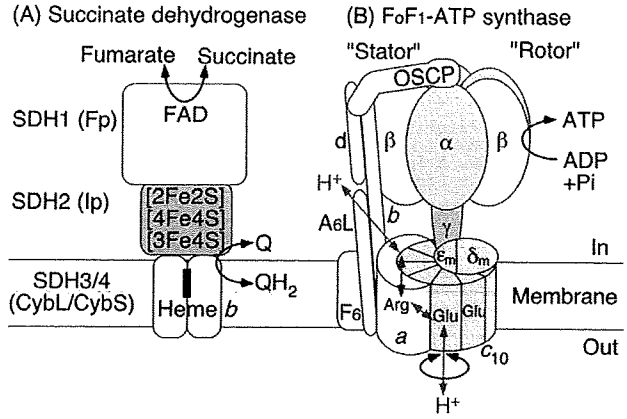

Fig. 2. Structure model for protist Complex II and ATP synthase.

the erythrocytic stage cells (Lasonder et al., 2008), sequence analysis of the anchor subunits was difficult in the *Plasmodium* mitochondria. Here we report candidates for the membrane anchor subunits of the *Plasmodium* oxidative phosphorylation enzymes. SDH3 and SDH4 of Complex II were identified by using structural fingerprints as probes while subunits *a* and *b* of ATP synthase were identified by BLAST search with proteomics data from other protists. Assignment of the membrane anchors of *Plasmodium* Complex II and ATP synthase will help our understanding of energy metabolism and the development of new antimalarials.

2. Materials and methods

2.1. Analytical methods

The presence of structural fingerprints (i.e., the heme/quinone-binding motifs) in ORFs shared by *P. falciparum* and *P. y. yoelii* genomes in the TIGR Parasite Database (http://www.tigr.org/tdb/e2k1/pya1/pya1-ortho.shtml/) was examined manually. Database searches using protein sequences were performed with the BLAST service at NCBI (http://www.ncbi.nlm.nih.gov/), GeneDB (http://www.genedb.org/), PlasmoDB (http://plasmodb.org/plasmo/), and TBestDB (http://tbestdb.bcm.umontreal.ca/). Sequences were aligned with ClustalX 2.0 (Larkin et al., 2007) and manual adjustments were made if needed. Transmembrane regions were identified with TMHMM (http://www.cbs.dtu.dk/services/TMHMM/).

3. Results and discussion

3.1. Evidence for the presence of membrane anchors of Plasmodium Complex II

Mammalian Complex II belongs to type C Complex II (Hägerhäll, 1997) and consists of four subunits and is bound to the matrix side of the inner mitochondrial membrane (Cecchini, 2003). A flavoprotein subunit (Fp, SDH1) and an iron–sulfur subunit (Ip, SDH2) form a soluble heterodimer, which then binds to a membrane anchor *b*-type cytochrome (SDH3/SDH4 heterodimer). SDH1 contains a covalently bound FAD and transfers electrons from succinate to the iron–sulfur clusters in SDH2. Electrons are then transferred to ubiquinone within a binding pocket provided by SDH2 and the SDH3/SDH4 heterodimer (Yankovskaya et al., 2003; Sun et al., 2005; Yang et al., 1998; Horsefield et al., 2006). Bacterial and mitochondrial SDH3 and SDH4 generally consist of three transmembrane helices (TM) each (I–III and IV–VI, respectively) (Yankovskaya et al., 2003; Sun et al., 2005). The quinone/heme-binding motifs, "$RPx_{16}Sx_2HR$" in TM-I and "$Hx_{10}D$" in TM-II of SDH3 and "$Hx_{10}DY$" in TM-V of SDH4 can be identified by sequence comparisons (Figs. 3 and 4). Arg31 (*Escherichia coli* Complex II numbering) in the SDH3 Sx_2HR motif and Asp82 in the SDH4 $Hx_{10}DY$ motif are in close proximity to ubiquinone and could interact with Tyr83 (Yankovskaya et al., 2003). Ser27 in the SDH3 Sx_2HR motif has been shown to be essential for quinone binding (Yang et al., 1998) and is a candidate for hydrogen bonding to the O_4 atom of ubiquinone (Horsefield et al., 2006). Tyr83 in the SDH4 $Hx_{10}DY$ motif could hydrogen bond to the O_1 atom of ubiquinone and contribute to the binding affinity (Yankovskaya et al., 2003; Horsefield et al., 2006). Examination of the *E. coli* Complex II structure (PDB 1NEK) suggests that the first arginine (Arg9 in *E. coli* SDH3) in the $RPx_{16}Sx_3R$ motif is in the vicinity of Glu186 in SDH1 and Asp106 in SDH2 and may play a structural role through a hydrogen bond network. Histidines in helices II and V (His84 and His 71 in *E. coli* SDH3 and SDH4, respectively) serve as the axial ligands for heme *b* (Yankovskaya et al., 2003; Sun et al., 2005) (Fig. 4A) but are dispensable for assembly and quinone reduction (Tran et al., 2007; Oyedotun et al., 2007).

Earlier, we have cloned and sequenced genes coding for the *P. falciparum* SDH1 and SDH2 by homology probing (Takeo et al., 2000). In contrast to these subunits, *Plasmodium* SDH3 and SDH4 appear to be highly divergent from their mitochondrial orthologs and are not annotated in the current database at NCBI, GeneDB and PlasmoDB. The *P. falciparum* Complex II previously isolated from whole cell lysates was found to be the SDH1/SDH2 heterodimer with an apparent molecular weight of 90 kDa (Suraveratum et al., 2000). The authors claimed that *Plasmodium* Complex II has a much lower K_m (3 μM) for succinate than mammalian enzymes and has the plumbagin-sensitive succinate–quinone reductase activity. However, the concentration (0.2%) of the non-ionic detergent octyl glucoside used for the isolation of *P. falciparum* Complex II was insufficient to solubilize all membrane proteins (i.e., the critical micelle concentration of octyl glucoside is 0.73%). Octyl glucoside likely dissociates the SDH1/SDH2 dimer from the membrane anchors and the aerobic isolation of the SDH1/SDH2 dimer would likely damage the iron–sulfur clusters in SDH2. Thus, the enzyme activities of such preparations need to be carefully examined. Recently, we identified *P. y. yoelii* Complex II as a 135-kDa band by native PAGE followed by activity staining (Kawahara et al., 2009). 2D-PAGE analysis of the Complex II revealed the presence of two small subunits, candidates for *Plasmodium* SDH3 and SDH4. The succinate–quinone reductase activity of *P. falciparum* and *P. y. yoelii* mitochondria (Takashima et al., 2001; Mi-Ichi et al., 2005; Kawahara et al., 2009) and succinate respiration in rodent malaria mitochondria (Uyemura et al., 2000, 2004) support the presence of membrane anchor subunits of Complex II for transferring electron to ubiquinone molecule within the inner mitochondrial membrane.

3.2. Identification of Plasmodium Complex II anchor subunits

Protist SDH3 and SDH4 are generally divergent from their orthologs, so conventional BLAST programs using bacterial and eukaryotic sequences as queries failed to identify *Plasmodium* subunits in the current genome database. Recently, we purified Complex II from the parasitic protist *Trypanosoma cruzi* and identified six each of hydrophilic and hydrophobic subunits by protein sequencing (Morales et al., 2009). Supernumerary non-catalytic

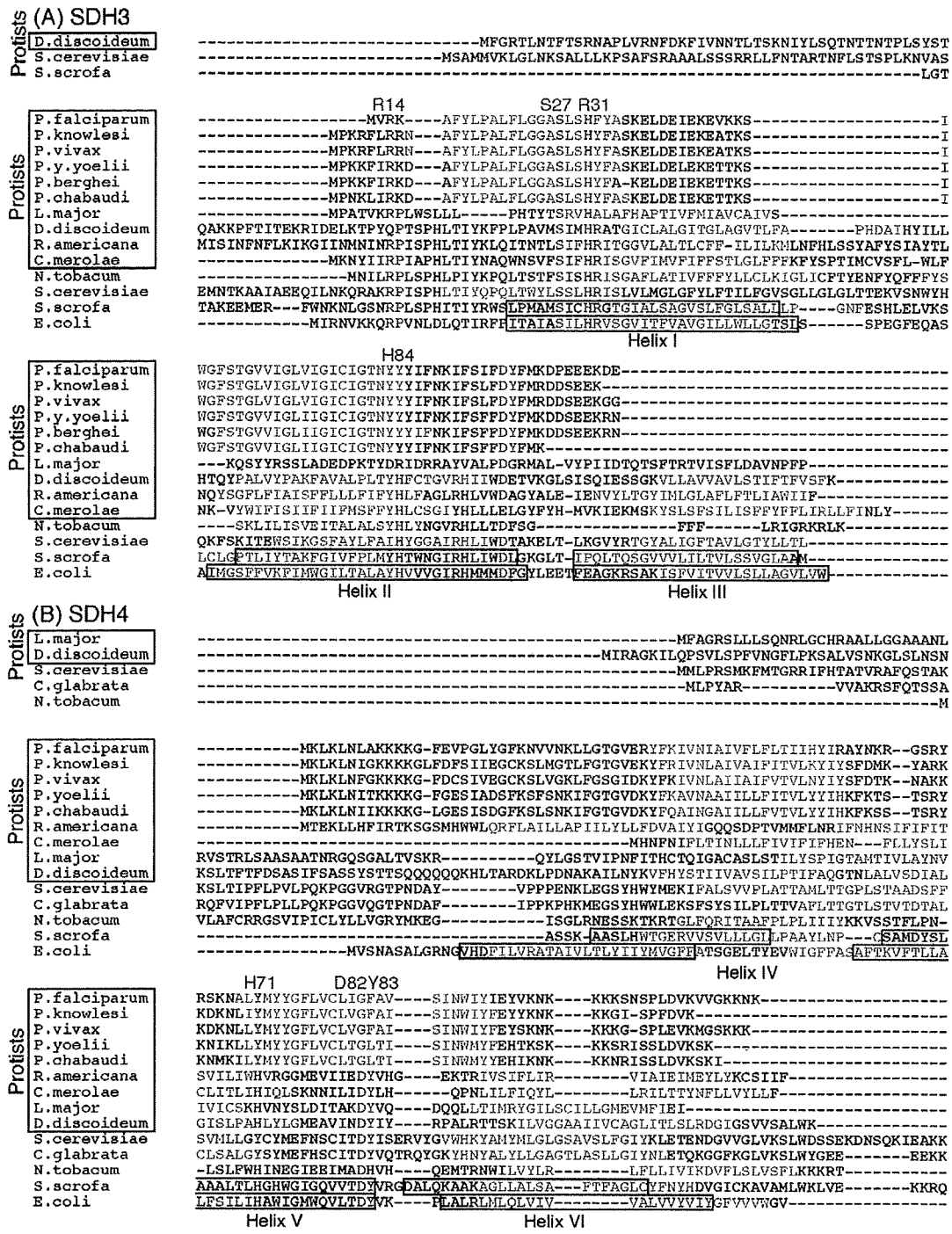

Fig. 3. Sequence alignment of SDH3 (A) and SDH4 (B) of *Plasmodium* Complex II. SDH3 and SDH4 sequences (GenBank accession Nos.) used are *P. falciparum* (XP_966100, XP_001347385), *P. knowlesi* (PKH_113810, PKH_080980), *P. vivax* (XP_001616129, XP_001614414), *P. y. yoelii* (XP_731082, XP_726783), *P. berghei* (XP_678526, not available), *P. chabaudi* (XP_742786, XP_738723), *Leishmania major* (XP_848167, XP_001685874), *Dictyostelium discoideum* (XP_643757, XP_642171), *Reclinomonas americana* (NP_044796, NP_044797), *Cyanidioschyzon merolae* (NP_059349, NP_059380), *Nicotiana tabacum* (YP_173376, YP_173457), *S. cerevisiae* S288C (NP_012781, NP_010463), *Candida glabrata* (not used, XP_446226), *Sus scrofa* (1ZOY_C, 1ZOY_D), and *E. coli* (NP_415249, NP_415250). Amino acid residues proposed for binding of ubiquinone and protoheme IX are shown in *red* and transmembrane regions predicted by TMHMM are in *blue*. Residue numbers refer to the *E. coli* SDH3 (SdhC) and SDH4 (SdhD) sequences. Transmembrane helices found in porcine Complex II (PDB 1ZOY) and *E. coli* Complex II (PDB 1NEK) are boxed.

subunits in *T. cruzi* Complex II may have evolved by complementary degeneration of dispersed duplicates (Hurles, 2004) in the Euglenozoa. Among six transmembrane subunits, we identified *T. cruzi* SDH3 and SDH4 on the basis of the presence of the quinone/heme-binding motifs, that are only conserved in these candidates (Morales et al., 2009).

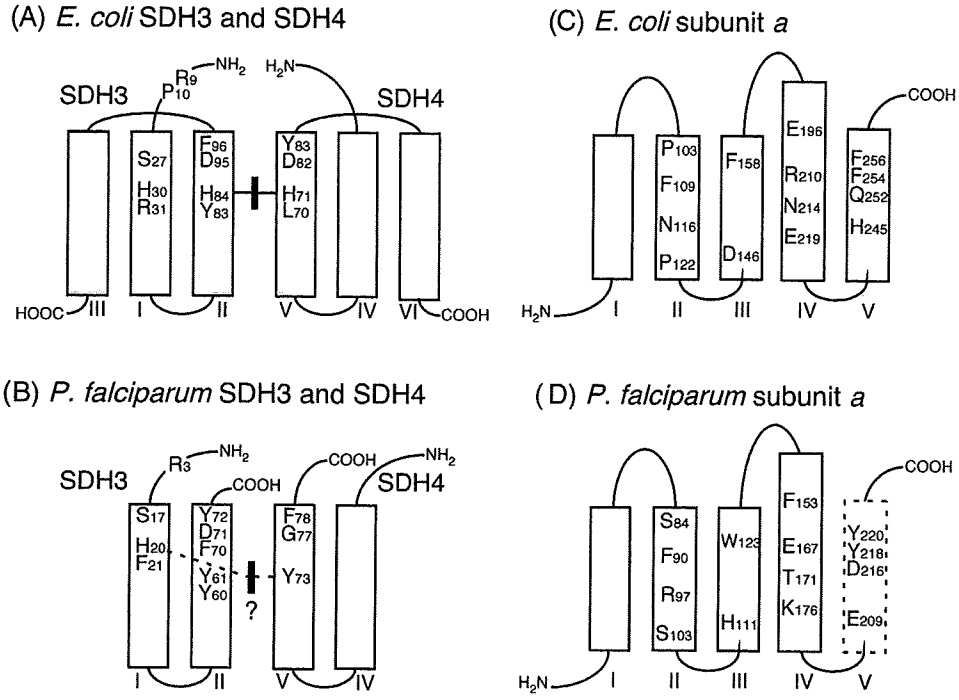

Fig. 4. Proposed structures for SDH3 and SDH4 of Complex II and subunits *a* from *E. coli* and *P. falciparum*.

Unlike *T. cruzi* mitochondria, the yield of *Plasmodium* mitochondria and the specific activity of Complex II were very low (Takashima et al., 2001; Mi-Ichi et al., 2005; Kawahara et al., 2009). Therefore, we took an alternative strategy for the identification of *Plasmodium* SDH3 and SDH4. We reexamined manually the sequences of *Plasmodium* membrane proteins for the presence of the quinone/heme-binding motifs of SDH3 and SDH4. Among 3310 ORFs[1] conserved in both *P. falciparum* and *P. y. yoelii* at the TIGR Parasite Database, 15.5% are membrane proteins with putative transmembrane segments, and 2.5% are shorter than 200 amino acid residues, as are the mitochondrial SDH3 and SDH4. From screening based on the number of TMs (1–3), spacing between TMs, conservation in *Plasmodium* spp., and the sequence motifs in transmembrane helices, we identified candidates for *P. falciparum* SDH3 (83 residues, GenBank accession No. XP_966100) and SDH4 (118 residues, XP_001347385) with two putative transmembrane helices (Figs. 3 and 4B, Table 1), which lack helices III and VI, respectively. Sequence identities of *P. falciparum* SDH3 and SDH4 against counterparts in *E. coli* and *Homo sapiens* are 15.7% and 14.3%, respectively, and 23.1% and 21.7%, respectively. An alternative candidate for PfSDH4 (XP_001349911 with one TM) contains the "YHx$_9$DY" motif but TMHMM predicts that this motif is in the C-terminal hydrophilic tail. Orthologs of PfSDH3 and PfSDH4 are present in human malaria parasites *Plasmodium vivax* and *Plasmodium knowlesi* and rodent malaria parasites *P. y. yoelii*, *Plasmodium berghei* and *Plasmodium chabaudi* in the current database[2]. Phylogenetic analysis of amino acid sequences showed that a clade for the membrane anchors of *Plasmodium* and Euglenozoa Complex II is an outgroup of bacterial and mitochondrial SDH3 and SDH4 (Fig. 5).

Table 1
Oxidative phosphorylation systems in *P. falciparum*.

Enzyme	Subunits	GenBank accession no.
NDH_2		XP_001352022
Succinate–quinone reductase	SDH1	XP_001347618
	SDH2	XP_001350535
	SDH3	XP_966100
	SDH4	XP_001347385
Ubiquinol:cytochrome *c* oxidoreductase	Cyt *b*	NP_059668[a]
	Rieske FeS	XP_001348547
	Cyt c_1	XP_001348771
	Hinge (QCR6)	XP_001348422
	MPP	XP_001351788, XP_001352201
Cytochrome *c*	Cyc1	XP_001348211
Cytochrome *c* oxidase	COX I	NP_059667[a] XP_001350328
	COX II	$(2_N)^b$, XP_001348462 $(2_C)^b$
	COX III	NP_059666[a]
	COX V	XP_001352148
	COX VI	XP_001352150
	COX VII	CAX64384
	COX VIII	XP_001351632
ATP synthase	ATP1 (α)	XP_001349675
	ATP2 (β)	XP_001350751
	ATP3 (γ)	XP_001349841
	ATP5 (OSCP, δ)	XP_001349828
	ATP16 (δ_m, ε)	XP_001348152
	ATP15 (ε_m)	XP_001349058
	ATP7 (d, p18)	XP_001348820
	ATP6 (*a*)	XP_001347344
	ATP4 (*b*)	XP_001348969
	ATP9 (*c*)	MAL7P1.340
Dihydroorotate dehydrogenase		XP_966023
NAD(P)-transhydrogenase		XP_001348682

[a] Heterodimeric COX II consist of two degenerated subunits, which retains the *N*- or *C*-terminal functional domain.

[1] Re-examination of the annotation of the *P. y. yoelii* genome on the basis of a detailed analysis of a comprehensive set of cDNA sequences and the liver stage proteome identified a further 510 genes which have orthologs in the *P. falciparum* genome (Vaughan et al., 2008). Analysis of these sequences did not yield any candidates for Complex II SDH3 and SDH4 and ATP synthase subunits *a* and *b*.

[2] The PbSDH3 sequence seems incomplete and the PbSDH4 sequence has not been identified yet at GeneDB. At NCBI, PfSDH3 was identified in *Toxoplasma gondiii* and the alternative PfSDH4 was found in other *Plasmodium* species, *T. gondii*, *Babesia bovis*, and *Theileria parva*.

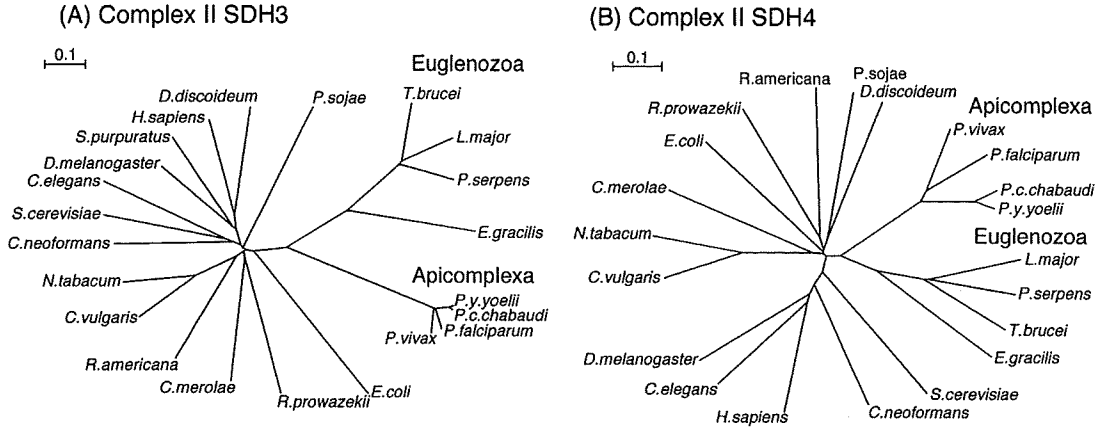

Fig. 5. Unrooted phylogenetic trees for SDH3 and SDH4 of Complex II. SDH3 and SDH4 sequences (GenBank accession Nos.) used are *H. sapiens* (NP_002992, NP_002993), *Caenorhabditis elegans* (NP_499283, NP_496369), *Cryptococcus neoformans* (XP_566692, XP_569088), *T. brucei* (XP_845531, XP_823384), *Phytomonas serpens* (CO723838, CO723900), *Euglena gracilis* (EC671331, EC610072), and *Rickettsia prowazekii* (NP_220518, NP_220519). All other sequences are described in the legend to Fig. 3.

3.3. Heme and quinone binding sites of Plasmodium Complex II

In *Plasmodium*, SDH3 contains an "$Rx_{13-14}Sx_2HY(F)$" motif in the *N*-terminal region of helix I and a "$YYx_{10}DY$" motif in the *C*-terminal region of helix II, in place of "$RPx_{16}Sx_2HR$" and "$YHx_{10}D$" motifs in other organisms (Figs. 3 and 4). *Plasmodium* SDH4 contains a "$Yx_{10}G$" motif in helix V in place of the canonical "$Hx_{10}DY$" motif (Figs. 3 and 4). Sequence alignments indicate that the tyrosines may substitute

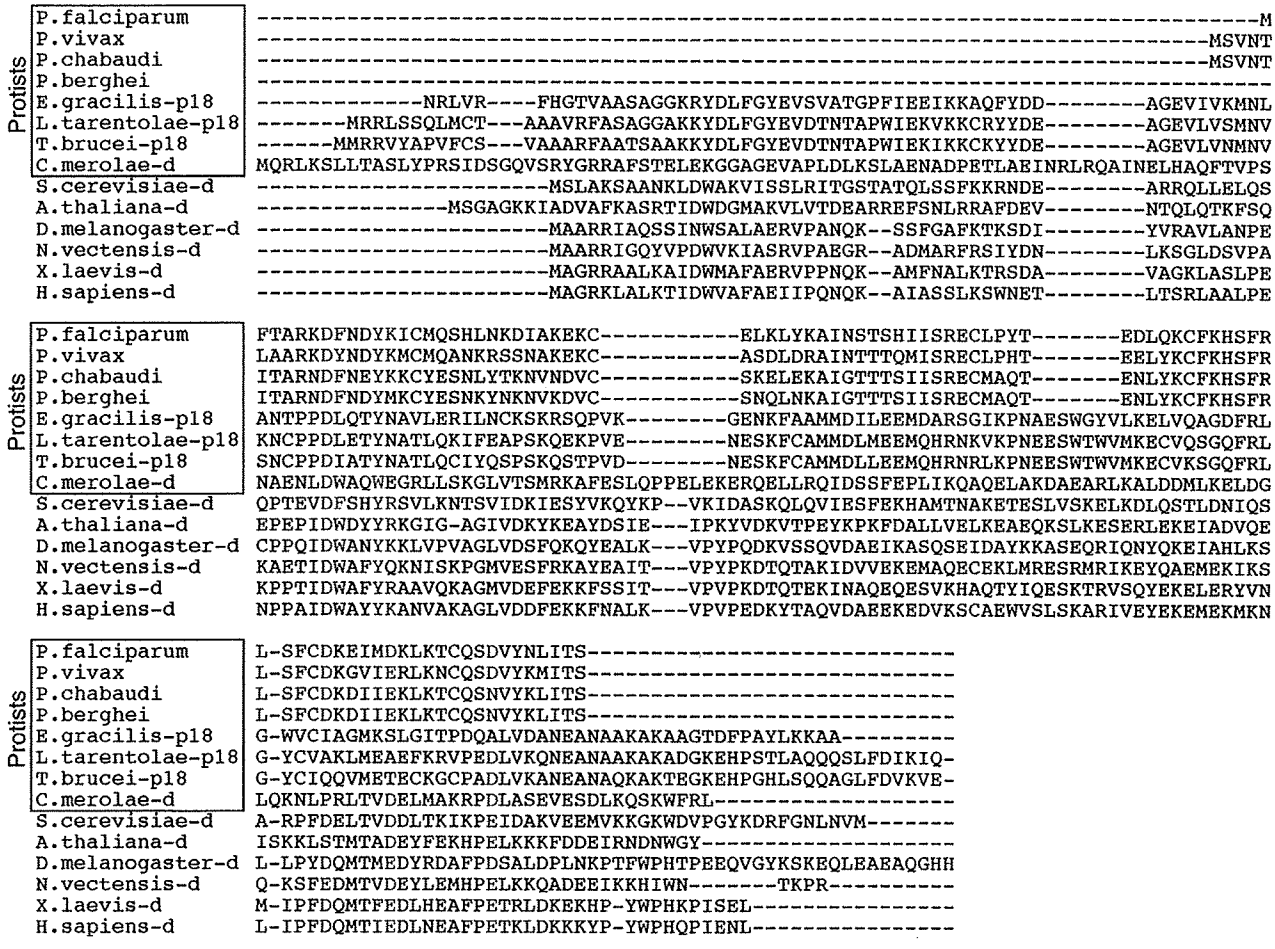

Fig. 6. Sequence alignment of subunit *d* (ATP7) of protist ATP synthase. Sequences used (GenBank accession No.) are *P. falciparum* (XP_001348820), *P. vivax* (PVX_117075), *P. c. chabaudi* (PCAS_133570), *P. berghei* (PB001416.02.0), *E. gracilis* (EC671747), *Leishmania tarentolae* (Q25423; p18), *T. brucei* (XP_844845; p18), *S. cerevisiae* (NP_012909), *Arabidopsis thaliana* (NP_190798), *Drosophila melanogaster* (NP_524402), *Nematostella vectensis* (XP_001626831), *Xenopus laevis* (NP_001084746), and *H. sapiens* (NP_006347). *C. merolae* subunit *d* sequence (CMK178C) was obtained at *Cyanidioschyzon merolae* Genome Project.

for Arg in the SDH3 "Sx_2HR" motif and histidines as heme ligands in SDH3 and SDH4 (Yankovskaya et al., 2003; Sun et al., 2005). It has been suggested that the role of a heme ligand in helix II (His84 in *E. coli* SDH3) could be replaced by a nearby histidine in the quinone-binding motif "Sx_2HR" in helix I (Maklashina et al., 2001). In SDH4 from *Saccharomyces cerevisiae* strain S288C (NP_010463) and rice (NP_001045324), the heme ligand His is substituted by Tyr and Gln, respectively. In catalase (Fita and Rossmann, 1985)

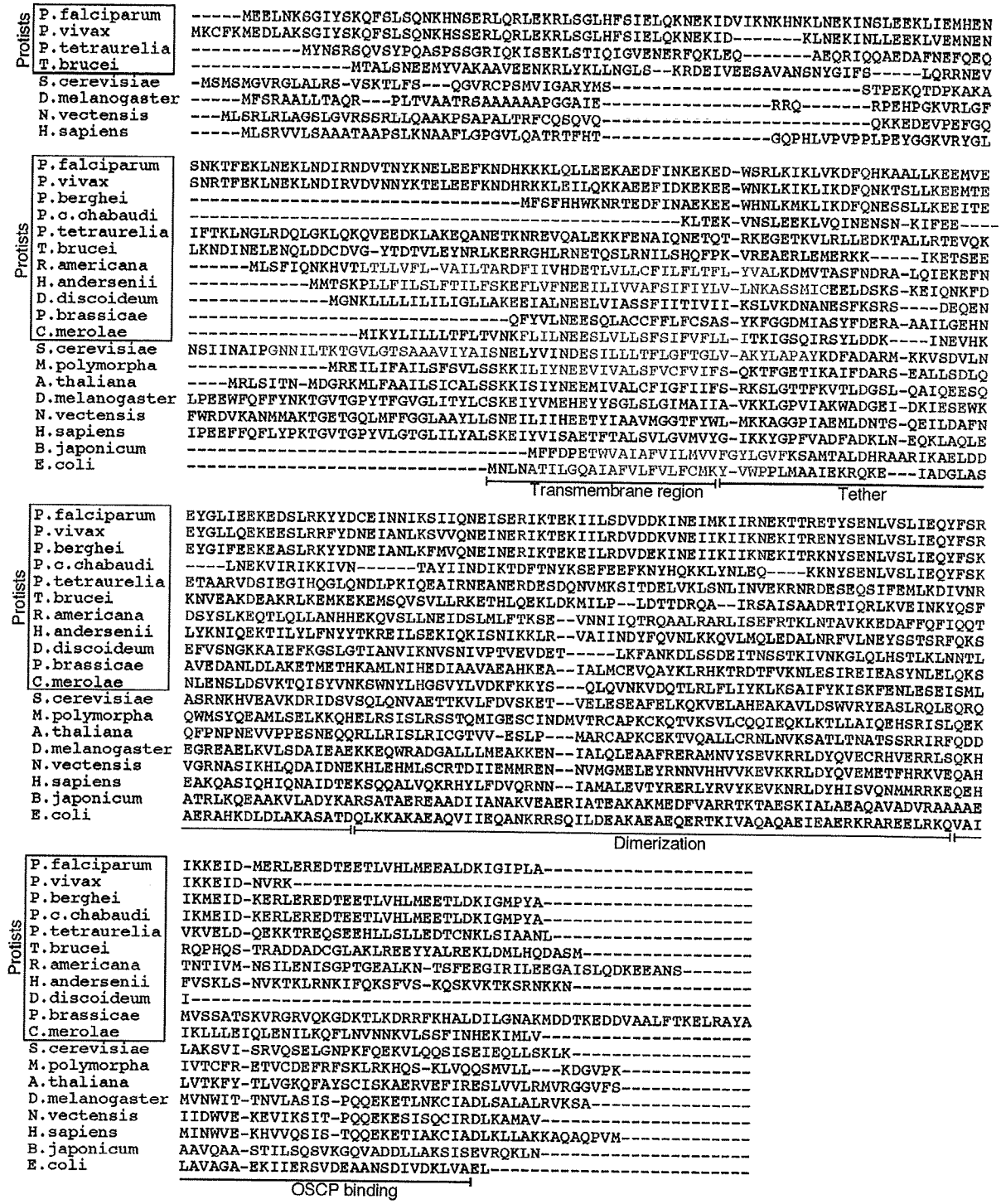

Fig. 7. Sequence alignment of subunit *b* (ATP4) of protist ATP synthase. Sequences used (GenBank accession No.) are *P. falciparum* (XP_001349752), *P. vivax* (XP_001613405), *P. berghei* (XP_680022), *P. c. chabaudi* (XP_743670), *Paramecium tetraurelia* (XP_001429993), *T. brucei* (XP_844845), *R. americana* (NP_044805), *Hemiselmis andersenii* (YP_001874763), *D. discoideum* (YP_001604088), *Phytophthora brassicae* (ES285372), *C. merolae* (NP_059355), *S. cerevisiae* (NP_015247), *Marchantia polymorpha* (NP_054459), *A. thaliana* (NP_085524), *D. melanogaster* (Q94516), *N. vectensis* (XP_001635800), *H. sapiens* (NP_001679), *Bradyrhizobium japonicum* (NP_767825), and *E. coli* (NP_418192). Domain structures shown are those proposed for *E. coli* AtpF (Dunn et al., 2000). Transmembrane helices predicted by TMHMM are indicated in *blue* and conserved residues are shown in *red*.

and other hemoproteins Tyr can coordinate the heme and the His-to-Tyr mutant of the yeast SDH3 "YHx$_{10}$D" motif retained half of the enzyme activity and heme content (Oyedotun and Lemire, 1999). In contrast to rhodoquinol–fumarate reductase (type C FRD) from parasitic nematodes (Saruta et al., 1995), menaquinol–fumarate reductase (type D FRD) from *E. coli* lacks heme *b* although membrane anchor subunits FrdC and FrdD have His and Cys, respectively, at the equivalent position of His84 and His71 of *E. coli* SdhC and SdhD, respectively (Hägerhäll, 1997; Cecchini, 2003). Depending on host environments, like *E. coli* FRD, *Plasmodium* Complex II may be able to catalyze both succinate oxidation and fumarate reduction despite *Plasmodium* mitochondria do not have low potential quinones. The presence or absence of the bound protoheme IX in *Plasmodium* Complex II and its enzymatic properties must be tested in future studies using the purified enzyme.

3.4. Membrane anchor subunits of Plasmodium ATP synthase

For a long time, it has been assumed that *Plasmodium* mitochondria cannot carry out oxidative phosphorylation (Fry and

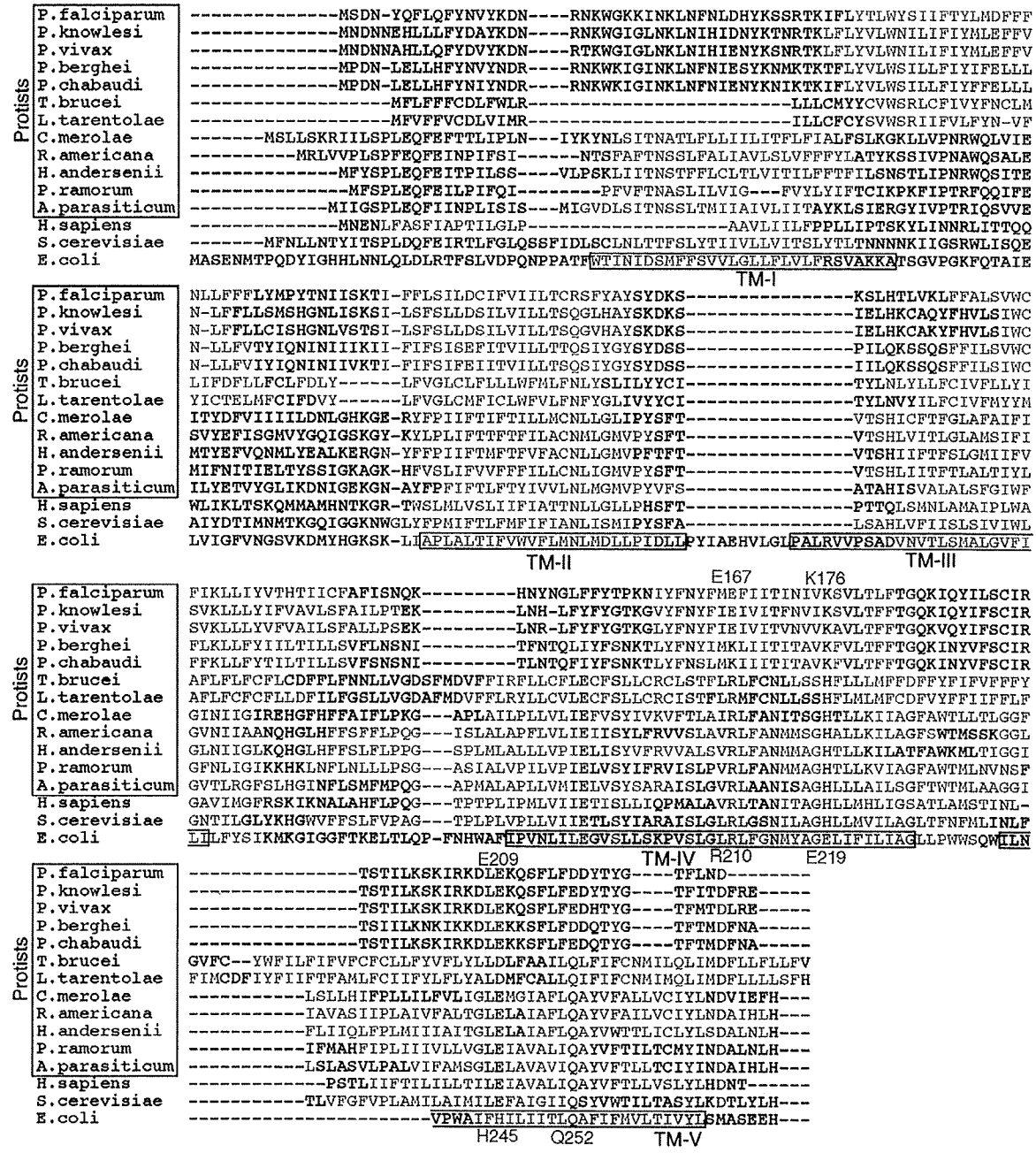

Fig. 8. Sequence alignment of subunit *a* (ATP6) of protist ATP synthase. Sequences used (GenBank accession No.) are *P. falciparum* (XP_001347344), *P. knowlesi* (CAQ39459), *P. vivax* (XP_001614365), *P. berghei* (XP_676120), *P. chabaudi* (XP_745940), *T. brucei* (AAA97428), *L. tarentolae* (AAA96695), *C. merolae* (NP_059364), *R. americana* (NP_044804), *H. andersenii* (YP_001874775), *D. discoideum* (NP_050086), *Phytophthora ramorum* (YP_001165346), *Amoebidium parasiticum* (AAN04079), *H. sapiens* (NP_536848), *S. cerevisiae* (CAA24054), and *E. coli* (NP_418194). Transmembrane helices (TM) predicted by TMHMM are indicated in *blue* and those proposed for *E. coli* AtpB (Moore et al., 2008) are boxed. Conserved amino acid residues in TM-IV and -V are shown in *red*.

Beesley, 1991) because of the apparent lack of transmembrane subunits *a* and *b* of the H^+-translocating F_oF_1-ATP synthase (Carlton et al., 2002; Gardner et al., 2002). However, oxidative phosphorylation in rodent malaria mitochondria (Uyemura et al., 2000, 2004) supports the presence of subunits *a* an *b* of the F_o subcomplex, which serve as the stator in the rotary mechanism (Noji et al., 1997; Fillingame et al., 2000) (Fig. 2), in *Plasmodium* ATP synthase.

Subunits *a* and *b* of protist ATP synthase are also highly divergent from bacterial and eukaryotic counterparts and are frequently not anotated in the database (Seeber et al., 2008). In mitochondrial genomes of land plants and certain protists, ORFs *ymf19* (*orfB*) and *ymf39* are conserved. Based on the sequence similarity and of mass spectrometric analysis, *Ymf19/OrfB* was assigned as subunit ATP8 (A6L) of the sunflower ATP synthase (Sabar et al., 2003). By protein sequencing and mass spectrometric analysis, Ymf39 was assigned as subunit *b* (ATP4 in mitochondria, AtpF in bacteria) in the jakobid *Seculamonas ecuadoriensis* (Burger et al., 2003), and the kinetoplastids *Crithidia fasciculata* (Speijer et al., 1997) and *Leishmania tarentolae* (Nelson et al., 2004). Based on peptide sequences of the *C. fasciculate* ATP synthase subunits, Allen et al. (2004) identified seven subunits of *Trypanosoma brucei* ATP synthase. By using these protist sequences as queries, we identified candidates for 10 subunits of *Plasmodium* ATP synthase with the current database (Table 1). In the mitochondrial ATP synthase, subunits *b* and ε of bacterial enzymes are split to subunits *b* and *d* and subunits δ_m and ε_m, respectively. We noticed that ATP16 (ε, δ_m) was mislabeled as ATP15 (ε_m) in *T. brucei* ATP synthase (Allen et al., 2004). Trypanosomatid p18 has been assigned as subunit *b* in previous studies (Nelson et al., 2004; Zíková et al., 2009). It is a hydrophilic nuclear gene product and our sequence analysis indicates that trypanosomatid and euglenid p18s are more closely related to subunit *d* (ATP7) (Devenish et al., 2000) (Fig. 6). As discussed by Burger et al. (2003), subunit *b* is rather featureless except for the locations of its transmembrane helices in the *N*-terminal region (Dunn et al., 2000) and there is no strictly conserved residue throughout species (Fig. 7).

Since the *C. fasciculate* band 3 homolog has four putative transmembrane helices, we tentatively assigned band 3 as subunit *a* (ATP6, AtpB) among four unassigned subunits of *T. brucei* ATP synthase (Allen et al., 2004). Using the *T. brucei* sequence as a query, we identified *Plasmodium* subunit *a* (Fig. 8). The sequence identities of *P. falciparum* subunit *a* with the *E. coli* AtpB (Fig. 4C) and *H. sapiens* ATP6 are 12.9% and 18.8%, respectively. TM-I of *Plasmodium* and *Trypanosoma* spp. showed a high sequence similarity and TM-IV and TM-V are conserved throughout species. Arg210 in transmembrane helix IV (*E. coli* AtpB numbering), which is essential for the proton translocation through the F_o subcomplex (Valiyaveetil and Fillingame, 1977; Fillingame et al., 2000; Moore et al., 2008), is substituted by Glu and Lys in human and rodent malaria parasites, respectively (Figs. 4D and 8). In *E. coli*, second site suppressor mutations of Arg210Gln in TM-IV have been identified as Gln252Arg and Gln252Lys in TM-V (Hatch et al., 1995; Ishmukhametov et al., 2008), indicating close proximity of these conserved residues. Notably, a pair of residues at positions 219 and 245 of *E. coli* subunit *a* are interchanged in mitochondria and the *E. coli* double mutant Glu219His/His245Glu was a slightly functional (Cain and Simoni, 1988). In the malaria parasites, Gln252 is replaced by Asp or Glu and Glu219 and His245 by Lys and Glu, respectively. Despite a lack of Arg210, a set of amino acid substitutions would make the *Plasmodium* subunit *a* functional.

In conclusion, here we identified candidates for six F_1 subunits [α, β, γ, δ (ATP5, OSCP), δ_m, and ε_m] and four F_o subunits (*a–d*) in *Plasmodium* spp (Table 1). Thus, the *Plasmodium* ATP synthase contains all eight subunits of the *E. coli* ATP synthase ($\alpha_3\beta_3\gamma_1\delta_1\varepsilon$-(=$\delta_m$ *plus* ε_m)$_1a_1b$(=*b plus d*)$_1c_{10?}$) and could carry out a rotary mechanism for ATP synthesis (Noji et al., 1997; Fillingame et al., 2000). Phylogenetic analysis showed that, in contrast to soluble catalytic subunit β (not shown), all three membrane anchor subunits, *a*, *b* (Fig. 9) and *c* (not shown), of *Plasmodium* and *Trypanosoma* spp. are divergent from their mitochondrial orthologs. Diversity in membrane anchors of parasitic protist mitochondrial ATP synthase suggests the plasticity in their structures even though they are essential for oxidative phosphorylation. Such variations may modulate or attenuate the function in host environments.

4. Conclusion and perspectives

We identified candidates for the membrane anchors of *Plasmodium* Complex II based on the presence of the structural fingerprints and showed sequence divergence from the eukaryotic orthologs. ATPase subunits *a* and *b* of *Plasmodium* were identified based on proteomics data of other protists, and again we found high sequence divergence in the membrane anchors. Our studies

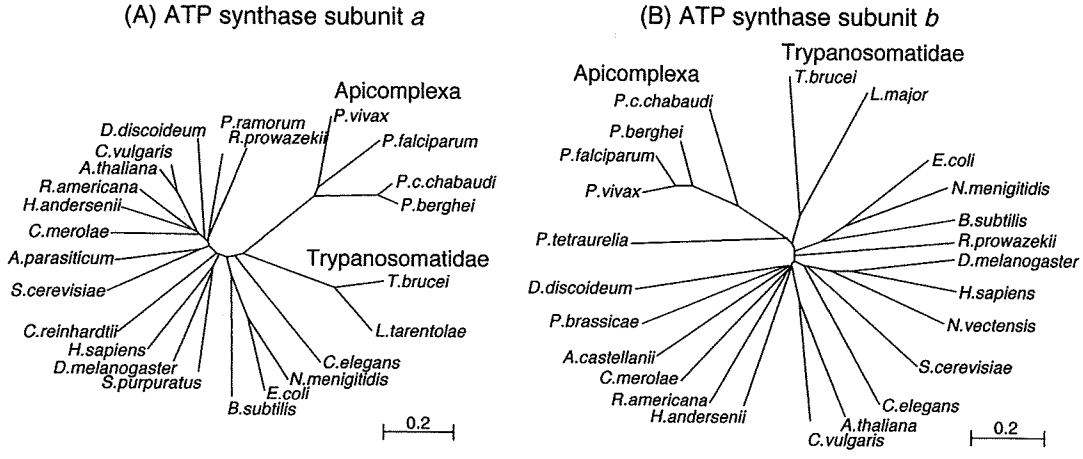

Fig. 9. Unrooted phylogenetic trees for subunit *a* (A) and *b* (B) of F-type ATP synthase. Subunits *a* and *b* sequences (GenBank accession Nos.) used are *D. melanogaster* (NP_008281, Q94516), *C. elegans* (NP_006956, NP_497938), *Strongylocentrotus purpuratus* (NP_006971, not available), *A. thaliana* (NP_085569, NP_085524), *Chara vulgaris* (NP_943689, NP_943702), *Chlamydomonas reinhardtii* (XP_001689492, not available), *L. major* (not available, XP_001686628), *Acanthamoeba castellanii* (not available, NP_042558), *R. prowazekii* (NP_220417, NP_220414), *Neisseria meningiditis* (NP_274934, NP_274932), and *Bacillus subtilis* (NP_391568, NP_391566). All other sequences were described in the legends to Figs. 7 and 8. The mitochondrial genomes encode eukaryotic subunits *a* except *C. reinhardtii* and *Plasmodium* spp. and subunit *b* of plants and some protists (*D. discoideum*, *C. merolae*, *R. americana*, and *H. andersenii*).

suggest that *Plasmodium* mitochondria possess all catalytic subunits for Complex II and ATP synthase (Table 1) and are fully capable of oxidative phosphorylation. Our approach is applicable to other membrane proteins although it is rather low throughput. Our assignments should help in understanding parasite energy metabolism.

Recently, diarylquinoline, a new tuberculosis-specific agent, has been shown to bind subunit *c* of ATP synthase (Andries et al., 2005). *Plasmodium* Complex II and ATP synthase could be pathogen-specific targets for new antimalarial agents, because of sequence divergence in membrane anchor subunits. In addition, alternative respiratory enzymes like NDH2 and malate:quinone oxidoreductase (MQO) are absent in mammalian mitochondria and are also promising targets. Since inhibitors for NDH2 are rare and mostly nonspecific (Kerscher, 2000), we screened natural antibiotics and identified gramicidin S and scopafungin as new inhibitors (Mogi et al., 2009). (Saleh et al., 2007) found that 1-hydroxy-2-dodecyl-4(1*H*)quinolone (HDQ), a potent inhibitor for yeast NDH2 (Eschemann et al., 2005), can act as an antimalarial. Even though our compounds were less effective on the *Plasmodium* enzyme than on bacterial enzymes, they may still serve as antimalarials. Such continuing efforts on the screening of natural and synthetic compounds could identify novel and potent drugs against malaria.

Acknowledgements

This study was supported by a grant-in-aid for scientific research (20570124 to TM) and Creative Scientific Research (18GS0314 to KK) from the Japan Society for the Promotion of Science, and a grant-in-aid for scientific research on Priority Areas (18073004 to KK) from the Ministry of Education, Culture, Sports, Science and Technology, Japan. We would like to thank Dr. B. Lemire (University of Alberta), Dr. G. Burger (University of Montreal), and Dr. S. Sato (National Institute for Medical Research, UK) for critical reading of the manuscript, Dr. M. Llinás (Princeton University), Dr. L. Lasonder, and Dr. H.E. Stunnenberg (Radboud University Nijmegen) for the use of their unpublished results.

References

Allen, J.W.A., Ginger, M.L., Ferguson, S.J., 2004. Maturation of the unusual single-cysteine (XXXCH) mitochondrial *c*-type cytochromes found in trypanosomatids must occur through a novel biogenesis pathway. Biochem. J. 383, 537–542.

Andries, K., Verhasselt, P., Guillemont, J., Göhlmann, H.W.H., Neefs, J.M., Winkler, H., Gestel, J.V., Timmerman, P., Zhu, M., Lee, E., Williams, P., de Chaffoy, D., Huitric, E., Hoffner, S., Cambau, E., Truffot-Pernot, C., Lounis, N., Jarlier, V., 2005. A diarylquinoline drug active on the ATP synthase of *Mycobacterium tuberculosis*. Science 307, 223–227.

Biagini, G.A., Viriyavejakul, P., O'Neill, P.M., Bray, P.G., Ward, S.A., 2006. Functional characterization and target validation of alternative Complex I of *Plasmodium falciparum* mitochondria. Antimicrob. Agents Chemother. 50, 1841–1851.

Burger, G., Lang, B.F., Braun, H.-P., Marx, S., 2003. The enigmatic mitochondrial ORF *ymf39* codes for ATP synthase chain *b*. Nucleic Acids Res. 31, 2353–2360.

Cain, B.D., Simoni, R.D., 1988. Interaction between Glu-219 and His-245 within the *a* subunit of F_1F_0-ATPase in *Escherichia coli*. J. Biol. Chem. 263, 6606–6612.

Carlton, J.M., Angiuoli, S.V., Suh, B.B., Kooij, T.W., Pertea, M., Silva, J.C., Ermolaeva, M.D., Allen, J.E., Selengut, J.D., Koo, H.L., Peterson, J.D., Pop, M., Kosack, D.S., Shumway, M.F., Bidwell, S.L., Shallom, S.J., van Aken, S.E., Riedmuller, S.B., Feldblyum, T.V., Cho, J.K., Quackenbush, J., Sedegah, M., Shoaibi, A., Cummings, L.M., Florensk, L., Yatesk, J.R., Raine, J.D., Sinden, R.E., Harris, M.A., Cunningham, D.A., Preiser, P.R., Bergman, L.W., Vaidya, A.B., van Lin, L.H., Janse, C.J., Waters, A.P., Smith, H.O., White, O.R., Salzberg, S.L., Venter, J.C., Fraser, C.M., Hoffman, S.L., Gardner, M.J., Carucci, D.J., 2002. Genome sequence and comparative analysis of the model rodent malaria parasite *Plasmodium yoelii yoelii*. Nature 419, 512–519.

Cecchini, G., 2003. Function and structure of Complex II of the respiratory chain. Annu. Rev. Biochem. 72, 77–109.

Daily, J.P., Scanfeld, D., Pochet, N., Roch, K.L., Plouffe, D., Kamel, M., Sarr, O., Mboup, S., Ndir, O., Wypij, D., Lavasseur, K., Thomas, E., Tamayo, P., Dong, C., Zhou, Y., Lander, E.S., Ndiaye, D., Wirth, D., Winzeler, E.A., Mesirov, J.P., Regev, A., 2007. Distinct physiological states of *Plasmodium falciparum* in malaria-infected patients. Nature 450, 1091–1095.

Devenish, R.J., Prescott, M., Roucou, X., Nagley, P., 2000. Insights into ATP synthase assembly and function through the molecular genetic manipulation of subunits of the yeast mitochondrial enzyme complex. Biochim. Biophys. Acta 1458, 428–442.

Dunn, S.D., McLachlin, D.T., Revington, M., 2000. The second stalk of *Escherichia coli* ATP synthase. Biochim. Biophys. Acta 1468, 356–363.

Eschemann, A., Galkin, A., Oettmeier, W., Brandt, U., Kerscher, S., 2005. HDQ (1-hydroxy-2-dodecyl-4(1*H*)quinolone), a high affinity inhibitor for mitochondrial alternative NADH dehydrogenase: evidence for a ping-pong mechanism. J. Biol. Chem. 280, 3138–3142.

Fillingame, R.H., Jiang, W., Dimitriev, O.Y., 2000. Coupling of H^+ transport to rotary catalysis in F-type ATP synthases: structure and organization of the transmembrane rotary motor. J. Exp. Biol. 203, 9–17.

Fita, I., Rossmann, M.G., 1985. The active center of catalase. J. Mol. Biol. 185, 21–37.

Foth, B.J., Stimmler, L.M., Handman, E., Crabb, B.S., Hodder, A.N., McFadden, G.I., 2005. The malaria parasite *Plasmodium falciparum* has only one pyruvate dehydrogenase complex, which is located in the apicoplast. Mol. Microbiol. 55, 39–53.

Fry, M., Webb, E., Pudney, M., 1990. Effect of mitochondrial inhibitors on adenosine triphosphate levels in *Plasmodium falciparum*. Comp. Biochem. Physiol. B 96, 775–782.

Fry, M., Beesley, J.E., 1991. Mitochondria of mammalian *Plasmodium* spp. Parasitology 102, 17–26.

Gardner, M.J., Hall, N., Fung, E., White, O., Berriman, M., Hyman, R.W., Carlton, J.M., Pain, A., Nelson, K.E., Bowman, S., Paulsen, I.T., James, K., Eisen, J.A., Rutherford, K., Salzberg, S.L., Craig, A., Kyes, S., Chan, M.S., Nene, V., Shallom, S.J., Suh, B., Peterson, J., Angiuoli, S., Pertea, M., Allen, J., Selengut, J., Haft, D., Mather, M.W., Vaidya, A.B., Martin, D.M., Fairlamb, A.H., Fraunholz, M.J., Roos, D.S., Ralph, S.A., McFadden, G.I., Cummings, L.M., Subramanian, G.M., Mungall, C., Venter, J.C., Carucci, D.J., Hoffman, S.L., Newbold, C., Davis, R.W., Fraser, C.M., Barrell, B., 2002. Genome sequence of the human malaria parasite *Plasmodium falciparum*. Nature 419, 498–511.

Hägerhäll, C., 1997. Succinate: quinone oxidoreductases. Variations on a conserved theme. Biochim. Biophys. Acta 1320, 107–141.

Hatch, L.P., Cox, G.B., Howitt, S.M., 1995. The essential arginine residue at position 210 in the *a* subunit of the *Escherichia coli* ATP synthase can be transferred to position 252 with partial retention of activity. J. Biol. Chem. 270, 29407–29412.

Henn, M.W., Schopf, R., Maier, W.A., Seitz, H.M., 1998. The amino acid composition of *Anopheles stephensi* (Diptera: Culicidae) infected with *Nosema algerae* (Microsporida: Nosematidae). J. Invertebr. Pathol. 71, 42–47.

Horsefield, R., Yankovskaya, V., Sexton, G., Whittingham, W., Shiomi, K., Ōmura, S., Byrne, B., Cecchini, G., Iwata, S., 2006. Structural and computational analysis of the quinone-binding site of Complex II (succinate–ubiquinone oxidoreductase). A mechanism of electron transfer and proton conduction during ubiquinone reeuction. J. Biol. Chem. 281, 7309–7316.

Hurles, M., 2004. Gene duplication: the genomic trade in spare parts. PLoS Biol. 2, 0900–0904.

Hyde, J.E., 2005. Drug-resistant malaria. Trends Parasitol. 21, 494–498.

Ishmukhametov, R.R., Pond, J.B., Al-Huqail, A., Galkin, M.A., Vik, S.B., 2008. ATP synthesis without R210 of subunit *a* in the *Escherichia coli* ATP synthase. Biochim. Biophys. Acta 1777, 32–38.

Kawahara, K., Mogi, T., Tanaka, T.Q., Hata, M., Miyoshi, H., Kita, K., 2009. Mitochondrial dehydrogenases in the aerobic respiratory chain of the rodent malaria parasite *Plasmodium yoelii yoelii*. J. Biochem. 145, 229–237.

Kerscher, S.J., 2000. Diversity and origin of alternative NADH:ubiquinone oxidoreductase. Biochim. Biophys. Acta 1459, 274–283.

Larkin, M.A., Blackshields, G., Brown, N.P., Chenna, R., McGettigan, P.A., McWilliam, H., Valentin, F., Wallace, I.M., Wilm, A., Lopez, R., Thompson, J.D., Gibson, T.J., Higgins, D.G., 2007. ClustalW2 and ClustalX version 2. Bioinformatics 23, 2947–2948.

Lasonder, E., Janse, C.J., van Gemert, G., Mair, G.R., Vermunt, A.M.W., Douradinha, B.G., van Noort, V., Huynen, M.A., Luty, A.J.F., Kroeze, H., Khan, S.M., Sauerwein, R.W., Waters, A.P., Mann, M., Stunnenberg, H.G., 2008. Proteomic profiling of *Plasmodium* sporozoite maturation identifies new proteins essential for parasite development and infectivity. PLoS Pathogens 4, e1000195.

Maklashina, E., Rothery, R.A., Weiner, J.H., Cecchini, G., 2001. Retention of heme in axial ligand mutants of succinate–ubiquinone oxidoreductase (Complex II) from *Escherichia coli*. J. Biol. Chem. 276, 18968–18976.

Mi-Ichi, F., Miyadera, H., Kobayashi, T., Takamiya, S., Waki, S., Iwata, S., Shibata, S., Kita, K., 2005. Parasite mitochondria as a target of chemotherapy: inhibitory effect of licochalcone A on the *Plasmodium falciparum* respiratory chain. Ann. NY. Acad. Sci. 1056, 46–54.

Mogi, T., Matsushita, K., Miyoshi, H., Ui, H., Shiomi, K., Ōmura, S., Kita, K., 2009. Identification of new inhibitors for alternative NADH dehydrogenase (NDH-II). FEMS Microbiol. Lett. 291, 157–161.

Moore, K.J., Angevine, C.M., Vincent, O.D., Schwem, B.E., Fillingame, R.H., 2008. The cytoplasmic loops of subunit a of *Escherichia coli* ATP synthase may participate in the proton translocation mechanism. J. Biol. Chem. 283, 13044–13052.

Morales, J., Mogi, T., Mineki, S., Takashima, E., Mineki, R., Hirawake, H., Sakamoto, K., Ōmura, S., Kita, K., 2009. Novel mitochondrial Complex II isolated from *Trypanosoma cruzi* is composed of twelve peptides including a heterodimeric Ip subunit. J. Biol. Chem. 284, 7255–7263.

Nelson, R.E., Aphasizheva, I., Falick, A.M., Nebohacova, M., Simpson, L., 2004. The I-complex in *Leishmania tarentolae* is an uniquely-structured F_1-ATPase. Mol. Biochem. Parasitol. 135, 221–224.

Noji, H., Yasuda, R., Yoshida, M., Kinosita, K., 1997. Direct observation of the rotation of F_1-ATPase. Nature 386, 299–302.

Oyedotun, K.S., Lemire, B.D., 1999. The *Saccharomyces cerevisiae* succinate–ubiquinone oxidoreductase. Identification of Sdh3p amino acid residues involved in ubiquinone binding. J. Biol. Chem. 274, 23956–23962.

Oyedotun, K.S., Sit, C.S., Lemire, B.D., 2007. The *Saccharomyces cerevisiae* succinate dehydrogenase does not require heme for ubiquinone reduction. Biochim. Biophys. Acta 1767, 1436–1445.

Painter, H.J., Morrisey, J.M., Mather, M.W., Vaidya, A.B., 2007. Specific role of mitochondrial electron transport in blood-stage *Plasmodium falciparum*. Nature 446, 88–91.

Sabar, M., Gagliardi, D., Balk, J., Leaver, C., 2003. ORFB is a subunit of F_1F_o-ATP synthase: insight into the basis of cytoplasmic male sterility in sunflower. EMBO Rep. 4, 381–386.

Saleh, A., Friesen, J., Baumeister, S., Gross, G., Bohne, W., 2007. Growth inhibition of *Toxoplasma gondii* and *Plasmodium falciparum* by nanomolar concentrations of 1-hydroxy-2-dodecyl-4(1*H*)quinolone, a high-affinity inhibitor of alternative (type II) NADH dehydrogenases. Antimicrob. Agents Chemother. 51, 1217–1222.

Saruta, F., Kuramochi, T., Nakamura, K., Takamiya, S., Yu, Y., Aoki, T., Sekimizu, K., Kojima, S., Kita, K., 1995. Stage-specific isoforms of complex II (succinate–ubiquinone oxidoreductase) in mitochondria from the parasitic nematode, *Ascaris suum*. J. Biol. Chem. 270, 928–932.

Seeber, F., Limenitakis, J., Soldati-Favre, D., 2008. Apicomplexan mitochondrial metabolism: a story of gains, losses and retentions. Trends Parasitol. 24, 468–478.

Sherman, I.W., 1998. Carbohydrate metabolism of asexual stages. In: Sherman, I.W. (Ed.), Malaria, Parasite Biology, Pathogenesis and Protection. ASM Press, Washington, DC, pp. 135–143.

Speijer, D., Breek, C.K., Muijsers, A.O., Hartog, A.F., Berden, J.A., Albracht, S.P., Samyn, B., van Beeumen, J., Benne, R., 1997. Characterization of the respiratory chain from cultured *Crithidia fasciculate*. Mol. Biochem. Parasitol. 85, 171–186.

Srivastava, I.K., Rottenberg, H., Vaidya, A.B., 1997. Atovaquone, a broad spectrum antiparasitic drug, collapses mitochondrial membrane potential in malarial parasite. J. Biol. Chem. 272, 3961–3966.

Sun, F., Huo, X., Zhai, Y., Wang, A., Xu, J., Su, D., Bartlam, M., Rao, Z., 2005. Crystal structure of mitochondrial respiratory membrane protein complex II. Cell 121, 1043–1057.

Suraveratum, N., Krungkrai, S.R., Leangaramgul, P., Prapunwattana, P., Krungkrai, J., 2000. Purification and characterization of *Plasmodium falciparum* succinate dehydrogenase. Mol. Biochem. Parasitol. 105, 215–222.

Takashima, E., Takamiya, S., Takeo, S., Mi-ichia, F., Amino, H., Kita, K., 2001. Isolation of mitochondria from *Plasmodium falciparum* showing dihydroorotate dependent respiration. Parasitol. Int. 50, 273–278.

Takeo, S., Kokaze, A., Ng, C.S., Mizuchi, D., Watanabe, J.I., Tanabe, K., Kojima, S., Kita, K., 2000. Succinate dehydrogenase in *Plasmodium falciparum* mitochondria: molecular characterization of the *SDHA* and *SDHB* genes for the catalytic subunits, the flavoprotein (Fp) and iron–sulfur (Ip) subunits. Mol. Biochem. Parasitol. 107, 191–205.

Tran, Q.M., Rothery, R.A., Maklashina, E., Cecchini, G., Weiner, J.H., 2007. *Escherichia coli* succinate dehydrogenase variant lacking the heme *b*. Proc. Natl. Acad. Sci. USA 104, 18007–18012.

Uyemura, S.A., Luo, S., Moreno, S.N.J., Docampo, R., 2000. Oxidative phosphorylation, Ca^{2+} transport, and fatty acid-induced uncoupling in malaria parasites mitochondria. J. Biol. Chem. 275, 9709–9715.

Uyemura, S.A., Luo, S., Vieira, M., Moreno, S.N., Docampo, R., 2004. Oxidative phosphorylation and rotenone-insensitive malate- and NADH-quinone oxidoreductases in *Plasmodium yoelii yoelii* mitochondria *in situ*. J. Biol. Chem. 279, 385–393.

Vaidya, A.B., Mather, M.W.A., 2005. Post-genomic view of the mitochondrion in malaria parasites. Curr. Top. Microbiol. Immunol. 295, 233–250.

Valiyaveetil, F.I., Fillingame, R.H., 1977. On the role of Arg-210 and Glu-219 of subunit *a* in proton translocation by the *Escherichia coli* F_oF_1-ATP synthase. J. Biol. Chem. 272, 32635–32641.

van Dooren, G.G., Stimmler, L.M., McFadden, G.I., 2006. Metabolic maps and functions of the *Plasmodium* mitochondrion. FEMS Microbiol. Rev. 30, 596–630.

Vaughan, A., Chiu, S., Ramasamy, G., Li, L., Gardner, M.J., Tarun, A.S., Kappe, S.H.I., Peng, X., 2008. Assessment and improvement of the *Plasmodium yoelii yoelii* genome annotation through comparative analysis. ISMB 24, i383–i389.

Yang, X., Yu, L., He, D., Yu, C.A., 1998. The quinone-binding site in succinate–ubiquinone reductase from *Escherichia coli*. Quinone-binding domain and amino acid residues involved in quinone binding. J. Biol. Chem. 273, 31916–31923.

Yankovskaya, V., Horsefield, R., Tornroth, S., Luna-Chavez, C., Miyoshi, H., Leger, C., Byrne, B., Cecchini, G., Iwata, S., 2003. Architecture of succinate dehydrogenase and reactive oxygen species generation. Science 299, 700–704.

Zíková, A., Schnaufer, A., Dalley, R.A., Panigrahi, A.K., Stuart, K.D., 2009. The F_oF_1-ATP synthase complex contains novel subunits and is essential for procyclic *Trypanosoma brucei*. PLoS Pathogens 5, e1000436.

Acta Crystallographica Section F
Structural Biology and Crystallization Communications
ISSN 1744-3091
Editors: **H. M. Einspahr and M. S. Weiss**

Crystallization and preliminary X-ray analysis of aspartate transcarbamoylase from the parasitic protist *Trypanosoma cruzi*

Kazuaki Matoba, Takeshi Nara, Takashi Aoki, Teruki Honma, Akiko Tanaka, Masayuki Inoue, Shigeru Matsuoka, Daniel Ken Inaoka, Kiyoshi Kita and Shigeharu Harada

Acta Cryst. (2009). F**65**, 933–936

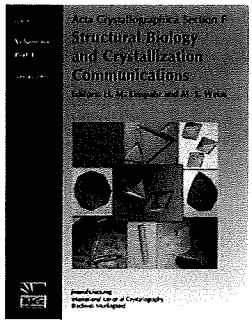

Acta Crystallographica Section F
Structural Biology and Crystallization Communications
ISSN 1744-3091

Crystallization and preliminary X-ray analysis of aspartate transcarbamoylase from the parasitic protist *Trypanosoma cruzi*

Kazuaki Matoba,[a] Takeshi Nara,[b] Takashi Aoki,[b] Teruki Honma,[c] Akiko Tanaka,[c] Masayuki Inoue,[d] Shigeru Matsuoka,[d] Daniel Ken Inaoka,[e] Kiyoshi Kita[e] and Shigeharu Harada[a]*

[a]Department of Applied Biology, Graduate School of Science and Technology, Kyoto Institute of Technology, Kyoto 606-8585, Japan, [b]Department of Molecular and Cellular Parasitology, Juntendo University School of Medicine, Tokyo 113-8421, Japan, [c]Systems and Structural Biology Center, RIKEN, Tsurumi, Yokohama 230-0045, Japan, [d]Graduate School of Pharmaceutical Sciences, The University of Tokyo, Tokyo 113-0033, Japan, and [e]Department of Biomedical Chemistry, Graduate School of Medicine, The University of Tokyo, Tokyo 113-0033, Japan

Correspondence e-mail: harada@kit.ac.jp

Received 23 April 2009
Accepted 12 August 2009

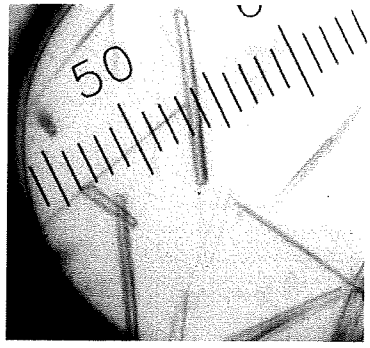

Aspartate transcarbamoylase (ATCase), the second enzyme of the *de novo* pyrimidine-biosynthetic pathway, catalyzes the production of carbamoyl aspartate from carbamoyl phosphate and L-aspartate. In contrast to *Escherichia coli* ATCase and eukaryotic CAD multifunctional fusion enzymes, *Trypanosoma cruzi* ATCase lacks regulatory subunits and is not part of the multifunctional fusion enzyme. Recombinant *T. cruzi* ATCase expressed in *E. coli* was purified and crystallized in a ligand-free form and in a complex with carbamoyl phosphate at 277 K by the sitting-drop vapour-diffusion technique using polyethylene glycol 3350 as a precipitant. Ligand-free crystals (space group $P1$, unit-cell parameters a = 78.42, b = 79.28, c = 92.02 Å, α = 69.56, β = 82.90, γ = 63.25°) diffracted X-rays to 2.8 Å resolution, while those cocrystallized with carbamoyl phosphate (space group $P2_1$, unit-cell parameters a = 88.41, b = 158.38, c = 89.00 Å, β = 119.66°) diffracted to 1.6 Å resolution. The presence of two homotrimers in the asymmetric unit (38 kDa × 6) gives V_M values of 2.3 and 2.5 Å^3 Da^{-1} for the $P1$ and $P2_1$ crystal forms, respectively.

1. Introduction

Chagas disease is a serious tropical disease that is endemic in Central and South America, affecting approximately 16–18 million people in these areas. The causative agent is a flagellate parasitic protist, *Trypanosoma cruzi*, which is transmitted by blood-feeding reduviid bugs. Manifestations of Chagas disease include severe cardiomyopathy, digestive injuries and neural disorders resulting from gradual tissue destruction caused by the parasite. Because nifurtimox and benznidazole, which are the currently used drugs for the treatment of Chagas disease, are toxic and ineffective in the chronic phase, the development of new chemotherapeutic drugs is urgently required (Urbina, 2002).

Pyrimidine biosynthesis is indispensable to all organisms and is achieved *via* the *de novo* and/or salvage pathways. *T. cruzi* possesses both pathways and their balance varies at different developmental stages of the parasite. Since the amastigote stage essentially relies on the *de novo* pathway (Gutteridge & Gaborak, 1979), in which uridine 5′-monophosphate is produced through a series of six enzymatic reactions, the enzymes of the *de novo* pathway therefore provide a greater potential as the primary targets of chemotherapy (Urbina & Docampo, 2003).

Aspartate transcarbamoylase (ATCase; EC 2.1.3.2), the second enzyme of the *de novo* pyrimidine-biosynthetic pathway, catalyzes the production of carbamoyl aspartate from carbamoyl phosphate (CP) and L-aspartate. *Escherichia coli* ATCase is a well known allosteric enzyme and is comprised of catalytic and regulatory subunits, the latter of which carries the binding site of the feedback inhibitor cytidine 5′-triphosphate (CTP; Gerhart & Pardee, 1964; Gerhart & Schachman, 1965; Shepherdson & Pardee, 1960). X-ray structural analysis of the *E. coli* enzyme demonstrated that the enzyme is composed of two trimers of the catalytic subunit (c) and three dimers of the regulatory subunit (r) to form a $(c_3)_2(r_2)_3$ quaternary structure (Krause *et al.*, 1985; Wiley *et al.*, 1972; Wiley & Lipscomb, 1968). ATCases from different strains of *Yersinia enterocolitica* and *Y. enterocolitica*-like organisms also exhibit the $(c_3)_2(r_2)_3$ structure but are sensitive to feedback inhibition by different

pyrimidine nucleotides (Foltermann *et al.*, 1981). *Bacillus subtilis* ATCase lacks the regulatory subunits (Stevens *et al.*, 1991) and in the hyperthermophile *Aquifex aeolicus* six ATCase chains noncovalently associate with six molecules of dihydroorotase (DHO), the third enzyme of the pyrimidine-biosynthetic pathway, to form a dodecamer (Zhang *et al.*, 2009).

On the other hand, eukaryotic ATCases from animals, fungi and Amoebozoa fuse with carbamoyl-phosphate synthetase II (CPS II; the first enzyme of the *de novo* pathway) and DHO to form a multifunctional fusion protein called CAD (Coleman *et al.*, 1977; Freund & Jarry, 1987; Simmer *et al.*, 1989; Souciet *et al.*, 1987), whose feedback inhibitor (CTP) binding site is located in the CPS II domain (Liu *et al.*, 1994). In contrast, *T. cruzi* ATCase (TcATCase), together with the ATCases from plants and other protists, is not part of the CAD multifunctional enzyme and is virtually insensitive to feedback inhibition by pyrimidine nucleotides (Aoki & Oya, 1987) since the enzyme lacks the regulatory subunit (El-Sayed *et al.*, 2005; Gao *et al.*, 1999). In addition, *N*-(phosphonoacetyl)-L-aspartate (PALA), a specific inhibitor of bacterial and mammalian ATCases (Aoki, 1994), only weakly inhibits TcATCase. Thus, structure determination of TcATCase, as well as of the other *de novo* pyrimidine-biosynthetic enzymes of *T. cruzi*, is considered to be crucial for the rational design of chemotherapeutic agents against Chagas disease.

Currently, the crystal structures of bacterial ATCases from *Escherichia coli* (Honzatko *et al.*, 1982), *Bacillus subtilis* (Stevens *et al.*, 1991), *Pyrococcus abyssi* (Van Boxstael *et al.*, 2003), *Sulfolobus acidocaldarius*, *Moritella profunda* (De Vos *et al.*, 2004, 2007) and *Methanococcus jannaschii* (Vitali & Colaneri, 2008), and of the *A. aeolicus* ATCase–DHO complex (Zhang *et al.*, 2009) have been reported. In the present study, we report the expression, purification, crystallization and preliminary X-ray analysis of TcATCase. This is the first crystallization report of an eukaryotic ATCase.

2. Materials and methods

2.1. Preparation of *T. cruzi* ATCase

The *T. cruzi* ATCase genes were previously cloned by screening the total DNA library of *T. cruzi* Tulahuen strain (Nara *et al.*, 2003). *T. cruzi* Tulahuen possesses three copies of the ATCase gene (*tcact1*, *tcact2* and *tcact3*, with GenBank accession Nos. AB074138, AB074139 and AB074140, respectively) and *tcact2* was selected for expression. The open reading frame of *tcact2* was amplified by PCR using 5′-CGGGATCCATGTTGGAACTGCCGCCAG-3′ and 5′-CGGG-ATCCTCACGCCAAAACGCTCCAC-3′ as the forward and reverse primers, respectively, and then subcloned into the bacterial expression vector pET14b (Novagen, EMD Biosciences Inc., Madison, Wisconsin, USA). The recombinant plasmid was introduced into *E. coli* BL21 (DE3) pLysS (Novagen). The transformant was grown in 1000 ml Luria–Bertani medium containing 50 μg ml^{-1} carbenicillin at 310 K until the absorbance at 600 nm (A_{600}) reached about 0.6. Expression of the recombinant His_6-tagged TcATCase was induced with 1 m*M* isopropyl β-D-1-thiogalactopyranoside at 310 K for 2 h. The cells were harvested by centrifugation at 5000*g* for 10 min and suspended in 20 ml lysis buffer (20 m*M* Tris–HCl pH 8.0, 0.5 *M* NaCl, 40 m*M* imidazole). After disruption of the cells by sonication, the lysate was centrifuged at 15 000*g* at 277 K for 20 min. The supernatant containing the His_6-tagged TcATCase was filtrated with a 0.22 μm pore-size filter and loaded onto a His-Trap FF column (1 ml bed volume; GE Healthcare) pre-equilibrated with lysis buffer. The column was then washed with 20 ml lysis buffer and the bound His_6-tagged TcATCase was eluted from the column with lysis buffer containing 500 m*M* imidazole. The fractions containing TcATCase were pooled and the buffer was exchanged to 20 m*M* Tris–HCl pH 7.4 using a PD-10 desalting column (GE Healthcare); they were then concentrated to 10 mg ml^{-1} with a centrifugal concentrator tube (Amicon Ultra-4 Ultracel-10K).

The ATCase activity was assayed by monitoring the production of carbamoyl aspartate from CP and L-aspartate by Ceriotti's colorimetric method (Prescott & Jones, 1969) with minor modifications. Briefly, 0.5 ml of a reaction mixture containing 200 m*M* Tris–HCl pH 7.9, 30 m*M* L-aspartate and purified ATCase was pre-incubated in a 1.5 ml quartz cuvette at 310 K for 5 min and the enzymatic reaction was then started by adding CP to a final concentration of 1.3 m*M*. CP was dissolved in ice-cold distilled water just before measurement. After standing for 15 min at 310 K, the reaction was stopped and 0.5 ml of a 1:1 mixture of 0.5% antipyrine in 50% sulfonic acid and 0.8% diacetylmonoxime in 5% acetic acid was added. Colorimetric development of the diazine produced from the carbamoyl aspartate and diacetylmonoxime was performed at 333 K for 2 h in the dark and the A_{466} was measured. The concentration of the carbamoyl aspartate produced was estimated from the A_{466} values of standard solutions containing carbamoyl aspartate at known concentrations. The typical specific activity of the purified TcATCase was 9 μmol min^{-1} mg^{-1} and the K_m values for CP and L-aspartate were estimated to be 0.03 and 29.4 m*M*, respectively.

TcATCase was purified to apparent homogeneity as shown by SDS–PAGE (Fig. 1), with a yield of about 2 mg from a 1000 ml culture. Gel-filtration chromatography with TSK-gel G3000SWXL (7.8 × 300 mm, Tosoh) and dynamic light-scattering analysis using DynaPro Titan (Wyatt Technology) both indicated that the purified enzyme existed as a homotrimer in solution.

2.2. Crystallization and X-ray data collection

All crystallization experiments were performed by the sitting-drop vapour-diffusion technique in 96-well Corning CrystalEX micro-

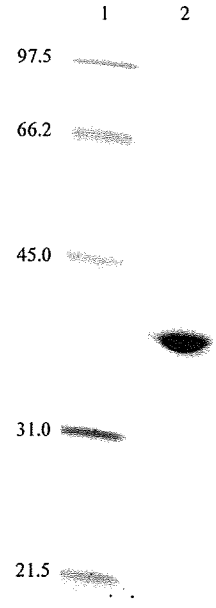

Figure 1
12.5% SDS–PAGE gel stained with Coomassie Brilliant Blue R-250 showing the apparent homogeneity of the purified TcATCase. Lane 1, molecular-weight markers (kDa); lane 2, TcATCase purified using a His-Trap FF column.

Table 1
Statistics of data collection and processing.

Values in parentheses are for the highest resolution shell.

	Ligand-free TcATCase	TcATCase–CP complex
Wavelength (Å)	0.900 (SPring-8 BL44XU)	1.000 (SPring-8 BL41XU)
Space group	$P1$	$P2_1$
Unit-cell parameters (Å, °)	a = 78.42, b = 79.28, c = 92.02, α = 69.56, β = 82.90, γ = 63.25	a = 88.41, b = 158.38, c = 89.00, β = 119.66
Solvent content† (%)	48	51
Frame number	222	180
Resolution range (Å)	50.0–2.8 (2.90–2.80)	50.0–1.60 (1.66–1.60)
No. of reflections	103124	946629
Unique reflections	44850	277190
Mosaicity	0.90	0.21
Redundancy	2.3 (2.3)	3.4 (3.4)
Completeness (%)	97.7 (98.4)	95.3 (91.4)
R_{merge}‡ (%)	7.4 (38.9)	6.5 (39.9)
Mean $I/\sigma(I)$	15.8 (4.4)	11.7 (3.9)

† Assuming the presence of six molecules in the asymmetric unit. ‡ $R_{merge} = \sum_{hkl}\sum_i |I_i(hkl) - \langle I(hkl)\rangle| / \sum_{hkl}\sum_i I_i(hkl)$, where $I_i(hkl)$ is the intensity of the ith observation of reflection hkl.

plates with a conical flat bottom (Hampton Research). In the initial screening for crystallization conditions, a 0.5 µl droplet containing around 10 mg ml^{-1} TcATCase dissolved in 20 mM Tris–HCl pH 7.4 was mixed with an equal volume of reservoir solution and the droplet was allowed to equilibrate against 100 µl reservoir solution at 277 and 293 K. Commercially available screening kits purchased from Hampton Research (Crystal Screen, Crystal Screen 2, Crystal Screen Lite and SaltRx) and Emerald BioStructures (Wizard I, Wizard II, Cryo I and Cryo II) were used as reservoir solutions. Of the 434 conditions screened, condition No. 10 from Crystal Screen Lite [15%(*w*/*v*) PEG 4000, 0.1 M sodium acetate pH 4.6, 0.2 M ammonium acetate] gave tiny plate-shaped crystals at 277 K. The condition was then optimized using 154 conditions by varying the PEG concentration (4–16%), the buffer pH (3.6–5.6) and the temperature (277 and 293 K) using PEG 3350, which is a monodisperse and high-purity polyethylene glycol obtained from Hampton Research, as a precipitant. For the best condition found, the effects of 72 additives on crystallization were examined using Additive Screen kits (Hampton Research) according to the manufacturer's instruction. Cobalt chloride and glycerol improved the size of the crystals; moreover, the addition of both additives gave thicker crystals. Currently, crystals larger than 0.2 × 0.1 × 0.01 mm can be grown at 277 K from reservoir solution containing 8–10%(*w*/*v*) PEG 3350, 0.1 M acetate buffer pH 4.6, 0.2 M ammonium acetate, 0.01 M cobalt chloride and 3% glycerol. For cocrystallization with CP, a freshly prepared 100 mM CP solution was added to the TcATCase solution to give a final concentration of 5 mM and crystallization was conducted as described above. Crystals of similar shape and size were obtained.

X-ray diffraction experiments were performed on the BL44XU beamline (λ = 0.900 Å; equipped with a Bruker DIP-6040 detector system) and the BL41XU beamline (λ = 1.000 Å; equipped with a Rayonix CCD MX225HE detector) at SPring-8 (Harima, Japan) and on the BL17A beamline (λ = 1.000 Å; equipped with an ADSC Quantum 270 detector) at Photon Factory (Tsukuba, Japan). A crystal mounted in a nylon loop was transferred and soaked briefly in reservoir solution supplemented with 20%(*w*/*v*) glycerol and then flash-cooled by rapidly submerging it in liquid nitrogen. Diffraction data were collected under cryocooled conditions at 100 K. Images were recorded with an oscillation angle of 1°, an exposure time of 1 s per frame and a crystal-to-detector distance of 150 mm and were processed with the *HKL*-2000 software package (Otwinowski & Minor, 1997).

3. Results and discussion

His_6-tagged TcATCase (38 kDa) could be purified to homogeneity by one-step purification using His-Trap FF column chromatography (Fig. 1). The molecular weight of the purified enzyme estimated by gel-filtration chromatography (134 kDa) and dynamic light scattering (102 kDa; R_h = 4.3 nm, polydispersity = 13.9%, mass = 100%) indicated that the enzyme probably exists as a homotrimer in solution.

Crystals of ligand-free TcATCase were obtained at 277 K from reservoir solution containing 8–10%(*w*/*v*) PEG 3350, 0.1 M acetate buffer pH 4.6, 0.2 M ammonium acetate, 0.01 M cobalt chloride and 3% glycerol and reached maximum dimensions within two weeks (Fig. 2*a*). TcATCase complexed with CP was also crystallized by the cocrystallization method under the same conditions within 2 d (Fig. 2*b*). Analyses of the symmetry and systematic absences in the recorded diffraction patterns indicated that the crystals of ligand-free TcATCase belonged to the triclinic space group $P1$, with unit-cell parameters a = 78.42, b = 79.28, c = 92.02 Å, α = 69.56, β = 82.90, γ = 63.25°, whereas those of TcATCase complexed with CP belonged to the monoclinic space group $P2_1$, with unit-cell parameters a = 88.41, b = 158.38, c = 89.00 Å, β = 119.66°. Assuming the presence of two His_6-tagged TcATCase trimers (6 × 38 kDa) in the asymmetric unit, the V_M values are 2.3 and 2.5 Å^3 Da^{-1} for the triclinic and monoclinic

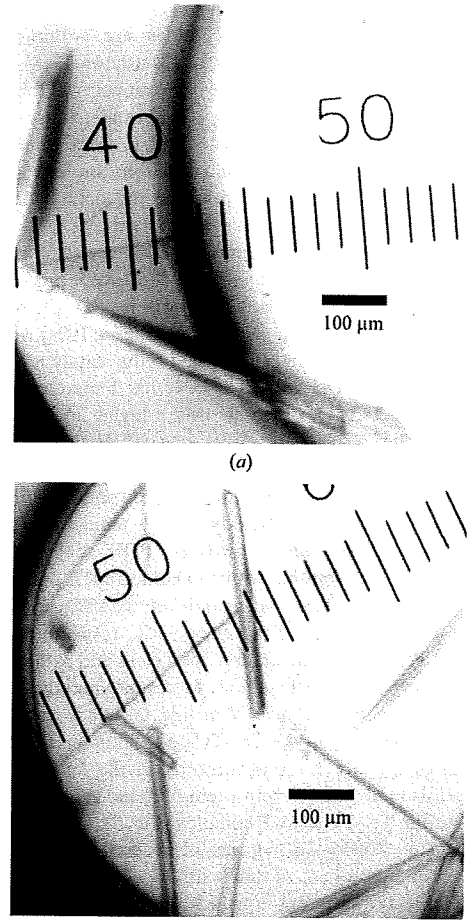

Figure 2
Crystals of (*a*) ligand-free TcATCase and (*b*) TcATCase complexed with carbamoyl phosphate obtained by the sitting-drop vapour-diffusion method using PEG 3350 as a precipitant.

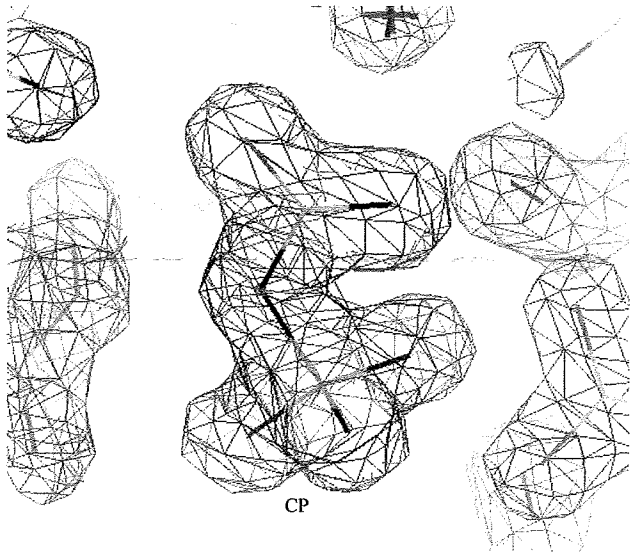

Figure 3
The $2F_o - F_c$ electron-density map around the bound CP in the TcATCase–CP complex structure contoured at 2σ. The structure is currently refined to $R = 0.151$ (1.6 Å resolution).

crystal forms, respectively; these values are within the range commonly observed for protein crystals (Matthews, 1968). A data set to 2.8 Å resolution (44 850 unique reflections) was obtained for ligand-free TcATCase after merging 103 124 reflections recorded on 222 images, while 277 190 unique reflections to 1.6 Å resolution were produced from 946 629 measured reflections on 180 images for TcATCase complexed with CP. Statistics of data collection and processing are shown in Table 1.

Attempts to solve the structures of both crystal forms by the molecular-replacement method with the *MOLREP* program (Vagin & Teplyakov, 1997) as implemented within the *CCP*4 package (Collaborative Computational Project, Number 4, 1994) were carried out using the homotrimeric structure of the catalytic subunit of *P. abyssi* ATCase (PDB code 1ml4; 40.1% amino-acid sequence identity with TcATCase), which showed a higher identity to TcATCase than to the ATCases from *E. coli* (PDB code 2atc; 36.5% identity), *B. subtilis* (PDB code 2at2; 32.5% identity), *S. acidocaldarius* (PDB code 2be9; 36.8% identity), *Moritella profunda* (PDB code 2be7; 37.7% identity), *Methanococcus jannaschii* (PDB code 2rgw; 38.6% identity) and *A. aeolicus* (PDB code 3d6n; 21.2% identity). A promising solution with two homotrimers per asymmetric unit was obtained for both the ligand-free TcATCase (correlation coefficient and R factor of 0.551 and 49.0%, respectively) and the TcATCase–CP complex (correlation coefficient and R factor of 0.615 and 50.9%, respectively). The models were subsequently subjected to rigid-body refinement and gave R factors of 44.8% and 44.4% for ligand-free TcATCase and the TcATCase–CP complex, respectively. Refinement of the structures is currently in the final stages. Clear electron densities for the entire protein part and the bound CP were observed for the TcATCase–CP complex (Fig. 3), but the loop of the CP-binding site (Cys85–Thr95) was disordered in the ligand-free TcATCase. The suppression of the flexibility of the loop by the bound CP may lead to the different crystal form and the enhanced X-ray diffraction of the crystals of the TcATCase–CP complex. We are now trying to prepare crystals of TcATCase complexed with potential inhibitors found in the Chemical Library of the Chemical Biology Research Initiative, University of Tokyo by *in silico* screening. Since the enzymes of the *de novo* pyrimidine-biosynthetic pathway have great potential as primary targets of chemotherapy (Urbina & Docampo, 2003), the detailed structures of TcATCase complexed with these compounds will help in structure-based drug design aimed at Chagas disease.

We thank all staff members of beamlines BL41XU and BL44XU at SPring-8 and BL17A at Photon Factory for their help with the X-ray diffraction experiments. This work was supported by a grant from the Targeted Proteins Research Program (TPRP) and was supported in part by a grant-in-aid for Creative Scientific Research (18GS0314 to KK) from the Japan Society for the Promotion of Science and a grant-in-aid for Scientific Research on Priority Areas (18073004) from the Japanese Ministry of Education, Science, Culture, Sports and Technology.

References

Aoki, T. (1994). *Jpn. J. Parasitol.* **43**, 1–10.
Aoki, T. & Oya, H. (1987). *Comput. Biochem. Physiol. B*, **87**, 143–150.
Coleman, P. F., Suttle, D. P. & Stark, G. R. (1977). *J. Biol. Chem.* **252**, 6379–6385.
Collaborative Computational Project, Number 4 (1994). *Acta Cryst.* D**50**, 760–763.
De Vos, D., Van Petegem, F., Remaut, H., Legrain, C., Glansdorff, N. & Van Beeumen, J. J. (2004). *J. Mol. Biol.* **339**, 887–900.
De Vos, D., Xu, Y., Hulpiau, P., Vergauwen, B. & Van Beeumen, J. J. (2007). *J. Mol. Biol.* **365**, 379–395.
El-Sayed, N. M. *et al.* (2005). *Science*, **309**, 409–415.
Foltermann, K. F., Wild, J. R., Zink, D. L. & O'Donovan, G. A. (1981). *Curr. Microbiol.* **6**, 43–47.
Freund, J. N. & Jarry, B. P. (1987). *J. Mol. Biol.* **193**, 1–13.
Gao, G., Nara, T., Nakajima-Shimada, J. & Aoki, T. (1999). *J. Mol. Biol.* **285**, 149–161.
Gerhart, J. C. & Pardee, A. B. (1964). *Fed. Proc.* **23**, 727–735.
Gerhart, J. C. & Schachman, H. K. (1965). *Biochemistry*, **4**, 1054–1062.
Gutteridge, W. E. & Gaborak, M. (1979). *Int. J. Biochem.* **10**, 415–422.
Honzatko, R. B., Crawford, J. L., Monaco, H. L., Ladner, J. E., Ewards, B. F., Evans, D. R., Warren, S. G., Wiley, D. C., Ladner, R. C. & Lipscomb, W. N. (1982). *J. Mol. Biol.* **160**, 219–263.
Krause, K. L., Volz, K. W. & Lipscomb, W. N. (1985). *Proc. Natl Acad. Sci. USA*, **82**, 1643–1647.
Liu, X., Guy, H. I. & Evans, D. R. (1994). *J. Biol. Chem.* **269**, 27747–27755.
Matthews, B. W. (1968). *J. Mol. Biol.* **33**, 491–497.
Nara, T., Hirayama-Noguchi, Y., Gao, G., Murai, E., Annoura, T. & Aoki, T. (2003). *Int. J. Parasitol.* **33**, 845–852.
Otwinowski, Z. & Minor, W. (1997). *Methods Enzymol.* **276**, 307–326.
Prescott, L. M. & Jones, M. E. (1969). *Anal. Biochem.* **32**, 408–419.
Shepherdson, M. & Pardee, A. B. (1960). *J. Biol. Chem.* **235**, 3233–3237.
Simmer, J. P., Kelly, R. E., Scully, J. L., Grayson, D. R., Rinker, A. G. Jr, Bergh, S. T. & Evans, D. R. (1989). *Proc. Natl Acad. Sci. USA*, **86**, 4382–4386.
Souciet, J. L., Potier, S., Hubert, J. C. & Lacroute, F. (1987). *Mol. Gen. Genet.* **207**, 314–319.
Stevens, R. C., Reinisch, K. M. & Lipscomb, W. N. (1991). *Proc. Natl Acad. Sci. USA*, **88**, 6087–6091.
Urbina, J. A. (2002). *Curr. Pharm. Des.* **8**, 287–295.
Urbina, J. A. & Docampo, R. (2003). *Trends Parasitol.* **19**, 495–501.
Vagin, A. & Teplyakov, A. (1997). *J. Appl. Cryst.* **30**, 1022–1025.
Van Boxstael, S., Cunin, R., Khan, S. & Maes, D. (2003). *J. Mol. Biol.* **326**, 203–216.
Vitali, J. & Colaneri, M. J. (2008). *Acta Cryst.* F**64**, 776–780.
Wiley, D. C., Evans, D. R., Warren, S. G., McMurray, C. H., Edwards, B. F., Franks, W. A. & Lipscomb, W. N. (1972). *Cold Spring Harb. Symp Quant. Biol.* **36**, 285–290.
Wiley, D. C. & Lipscomb, W. N. (1968). *Nature (London)*, **218**, 1119–1121.
Zhang, P., Martin, P. D., Purcarea, C., Vaishnav, A., Brunzelle, J. S., Fernando, R., Guy-Evans, H. I., Evans, D. R. & Edwards, B. F. (2009). *Biochemistry*, **48**, 766–778.

FEBS Letters 583 (2009) 1446–1450

ELSEVIER

FEBS Letters

journal homepage: www.FEBSLetters.org

The *Plasmodium* HU homolog, which binds the plastid DNA sequence-independent manner, is essential for the parasite's survival

Narie Sasaki [a,b], Makoto Hirai [c], Katsura Maeda [b], Ryoko Yui [a], Kie Itoh [d], Syoko Namiki [a], Teppei Morita [a], Masayuki Hata [e], Kimiko Murakami-Murofushi [b], Hiroyuki Matsuoka [c], Kiyoshi Kita [e], Shigeharu Sato [f,*]

[a] *Division of Biological Science, Graduate School of Science, Nagoya University, Nagoya 464-8602, Japan*
[b] *Department of Biology, Faculty of Science, Ochanomizu University, Tokyo 112-0012, Japan*
[c] *Division of Medical Zoology, Department of Infection and Immunity, Jichi Medical University School of Medicine, Shimotsuke 329-0498, Japan*
[d] *Department of Integrated Biosciences, Graduate School of Frontier Sciences, University of Tokyo, 5-1-5 Kashiwanoha, Kashiwa 277-8562, Japan*
[e] *Department of Biomedical Chemistry, Graduate School of Medicine, The University of Tokyo, Tokyo 113-0033, Japan*
[f] *Division of Parasitology, MRC National Institute for Medical Research, London NW7 1AA, UK*

ARTICLE INFO

Article history:
Received 27 February 2009
Revised 26 March 2009
Accepted 31 March 2009
Available online 7 April 2009

Edited by Michael Ibba

Keywords:
DNA binding protein
HU
Knock-out
Plastid
Plasmodium berghei
Plasmodium falciparum

ABSTRACT

The nuclear genome of the human malaria parasite *Plasmodium falciparum* encodes a homolog of the bacterial HU protein (PfHU). In this study, we characterised PfHU's physiological function. PfHU, which is targeted exclusively to the parasite's plastid, bound its natural target – the plastid DNA – sequence-independently and complemented lack of HU in *Escherichia coli*. The HU gene could not be knocked-out from the genome of *Plasmodium berghei*, implying that HU is important for the parasite's survival. As the human cell lacks the HU homolog, PfHU is a potential target for drugs to control malaria.

1. Introduction

Apicomplexan parasites such as the human malaria parasite *Plasmodium falciparum* have a vestigial secondary plastid that is often called the apicoplast [1]. Despite being non-photosynthetic, the apicomplexan plastid is indispensable for the parasite because the organelle is involved in essential metabolism such as isoprenoid biosynthesis [2]. The *P. falciparum* plastid contains its own genomic DNA which is 35 kb in size and extremely rich in A + T (86%) [1]. Almost all proteins encoded by the plastid DNA (ptDNA) are involved in either transcription or translation. Nevertheless, the plastid genome encodes at least one gene whose expression is critical for the parasite's survival, and drugs affecting bacterial type gene expression often cause the delayed death phenotype of the parasite [3].

In the plastid, genomic DNA is assembled into a compact, highly organised structure, the nucleoid [4], like in bacteria from which the plastid has evolved. Bacterial nucleoid formation depends on a group of bacterial histone-like DNA binding proteins (BHLs). The HU protein, which binds DNA in a sequence non-specific manner and bends the bound DNA, is the most abundant BHL in the bacterial cell [5]. *Escherichia coli* HU is a heterodimer of two highly homologous subunits HUα and HUβ, which are encoded by *hupA* and *hupB*, respectively [6]. HU is ubiquitously distributed among bacteria and this suggests that the protein is critical in bacterial nucleoid formation. In addition to an architectural role, HU is also involved in other cellular functions such as initiation of replication [7], transcriptional regulation [8] and DNA recombination [9] in *E. coli*.

Although the plastids of the photosynthetic eukaryotes are descendents of bacteria, their original, bacterial components have been gradually replaced to eukaryotic factors of equivalent function during the course of evolution. Today, the plastid HU homolog is only found in some algal species and apicomplexans [4]. The algal HUs such as those of *Cyanidioschyzon merolae* [10] and *Guillardia theta* [11] are capable of rescuing bacterial HU null mutants

Abbreviations: BHL, bacterial histone-like DNA binding protein; ptDNA, plastid DNA

* Corresponding author. Fax: +44 20 8816 2730.
E-mail address: ssato@nimr.mrc.ac.uk (S. Sato).

0014-5793/$36.00
doi:10.1016/j.febslet.2009.03.071

from its abnormal phenotype. The HU of *G. theta* bends DNA to which it binds [11], suggesting that this protein is critical in the formation of the nucleoid in this alga's plastid.

Recently, Ram et al. reported that the nuclear genome of *P. falciparum* encodes a HU homolog (PfHU) that is probably involved in DNA compaction in the plastid [12]. They found PfHU doesn't exhibit the DNA-bending activity in vitro and attributed this to the fact that the protein lacks the highly conserved proline residue at the position corresponding to P63 of *E. coli* HUα.

In this study, we investigated how PfHU binds the plastid DNA, whether the protein complements lack of HU in an *E. coli* null mutant, and whether HU protein is essential in the related rodent malaria parasite *P. berghei*, in order to characterise the physiological function of PfHU.

2. Materials and methods

2.1. DNA-mobility shift assay

The Recombinant PfHUs, PfHU53-189 and PfHU53-148 were prepared as described in Supplementary material. DNA fragments A1280, A1838, B1624 and B1880 were PCR-amplified from the parasite's ptDNA with a set of synthetic primers described by Singh et al. [13]; AB1677 was amplified with 5′-CTTTATATGGAGCTCGTCCT-3′ and 5′-CTGATTTATTACCTGTTGGT-3′. Fifty nanograms of each DNA fragment was incubated with each recombinant protein (0, 50, 100, 200, 400, and 800 ng) in the reaction buffer (20 mM Tris–HCl, pH 7.5, 0.4 mM EDTA, 20 mM NaCl, 0.4 mM DTT) for 3 h at room temperature before application to a 1% agarose gel and electrophoresis, then the gel was stained with ethidium bromide.

2.2. Complementation test

The *hupB*::Km^r locus of the HUβ$^-$ *E. coli* strain JR1671 was transduced to the HUα$^-$ strain JR1670 carrying *hupA*::Cm^r to generate a *hupAhupB* double mutant by P1 transduction [14]. A pQE50 (Qiagen)-base expression plasmid encoding PfHU53-189 without an affinity tag was constructed and the *hupAhupB* double mutant was transformed with a plasmid expressing the recombinant protein. The transformant was grown on LB supplemented with 50 μg/ml kanamycin and 50 μg/ml ampicillin. Neither chloramphenicol nor IPTG was added to the growth medium because the double mutant was sensitive to chroramphenicol [14] and the excess induction of PfHU53-189 was harmful for growth of the bacteria (data not shown).

2.3. Knock-out of the nuclear gene of Plasmodium berghei

To disrupt the HU gene of *P. berghei* (PB000792.02.0) through double-crossover homologous recombination, the plasmid pPbHU-KO was constructed from pBS-DHFR [15] following the method used to construct another targeting plasmid pPbGCS1-KO, which was successfully used to knock-out the GCS1 gene of the parasite [16] (details in Supplementary material). *P. berghei* ANKA clone 2.34 was separately transfected with pPbGCS1-KO or pPbHU-KO by electroporation, and recombinant parasites were selected with pyrimethamine.

3. Results

3.1. PfHU binds the plastid DNA sequence-independently

Ram and colleagues reported that PfHU exhibits the DNA binding activity that is predictable from the presence of a complete BHL domain in the protein [12]. They also reported that PfHU is localised to the plastid [12]. We confirmed the plastid-specific location of the protein by immuno-fluorescence microscopy using the anti-PfHU antibody (Supplementary Fig. S1). Therefore, the organellar genomic DNA in the plastid is the only natural target of the binding of PfHU. Ram and colleagues carried out chromatin immuno-precipitation (ChIP) assays and suggested that PfHU binds at least part of the organellar DNA [12], but no further analysis has been done. Thus, in order to characterise the physiological function of PfHU in detail, we analysed the protein's binding to different parts of the ptDNA by DNA-mobility shift assay using the recombinant protein.

Transfection experiments using yellow fluorescent protein (YFP) fused to Met1-Met82 of PfHU (PfHU-YFP) showed that the N-terminal sequence functions as the plastid targeting sequence (Supplementary Fig. S2). We prepared two differently truncated forms of the recombinant PfHU, PfHU53-189 and PfHU53-148; PfHU53-189 lacks the N-terminal unconserved sequence (M1-I52) whereas PfHU53-148 contains only the BHL domain (Fig. 1A). The apparent molecular mass of PfHU53-189 determined by Western blotting is almost the same as the natural PfHU present in the parasite (Supplementary Fig. S3). This suggests that the unconserved N-terminal sequence is removed from the mature form of PfHU, which is almost the same as PfHU53-189, when the protein is targeted to the plastid.

For this analysis, we selected five different regions of the ptDNA (Fig. 1B). Four of them – A1838, A1820, B1624 and B1880 – were chosen from those described in the previous report by Singh et al [13], as they are in close proximity of the DNA replication initiation sites (A1820), protein coding regions with tRNA genes' cluster (B1624 and B1880) and a part of a protein coding gene (A1838), respectively. In addition, another region AB1677, which contains the ends of both the two gene clusters, was selected as it is supposed to be important in termination of transcription.

A PCR fragment of each region was incubated with PfHU53-189 and separated by agarose gel electrophoresis (Fig. 1C). The result clearly showed that the protein affected the mobility of all the five fragments. Shift of the band was apparent even at a protein/DNA mass ratio = 1 but it was much more prominent when the ratio was higher. The protein added at the same mass ratio affected the mobility of each fragment equally. This indicates that PfHU53-189 binds these five DNA fragments regardless of their size and nucleotide sequence. This suggests that PfHU binds the ptDNA sequence without specificity.

Another experiment with PfHU53-148, which consists of only the BHL domain of PfHU, showed that this shorter form also binds the ptDNA sequence-independently, though the protein's affinity for each fragment seemed to be lower than that of PfHU53-189 (Fig. 1D). This implies that the BHL domain is sufficient for PfHU to bind the DNA and the unique C-terminal sequence stabilises the DNA–protein complex.

3.2. PfHU complements the HU-deficient E. coli mutant

Although neither of the two genes (*hupA* and *hupB*) encoding the two subunits of HU is essential for the survival of *E. coli* on LB at 37 °C, *hupAhupB* double mutants exhibit characteristic phenotypes such as filamentous morphology and sensitivity to the cold [17]. To characterise the function of PfHU further, a *hupAhupB* double mutant strain was transformed with the expression plasmid for PfHU53-189 and the effect of the expressed recombinant protein on the mutant's phenotypes investigated.

Unlike the HU$^+$ parent strain JR1669 that is short and homogeneous in size, the *hupAhupB* double mutant exhibits a characteristic filamentous phenotype (Fig. 2A). On the LB plate, the mutant forms visible colonies at 37 °C, but no visible colony is formed at 25 °C (Fig. 2B). By contrast, the transformants expressing

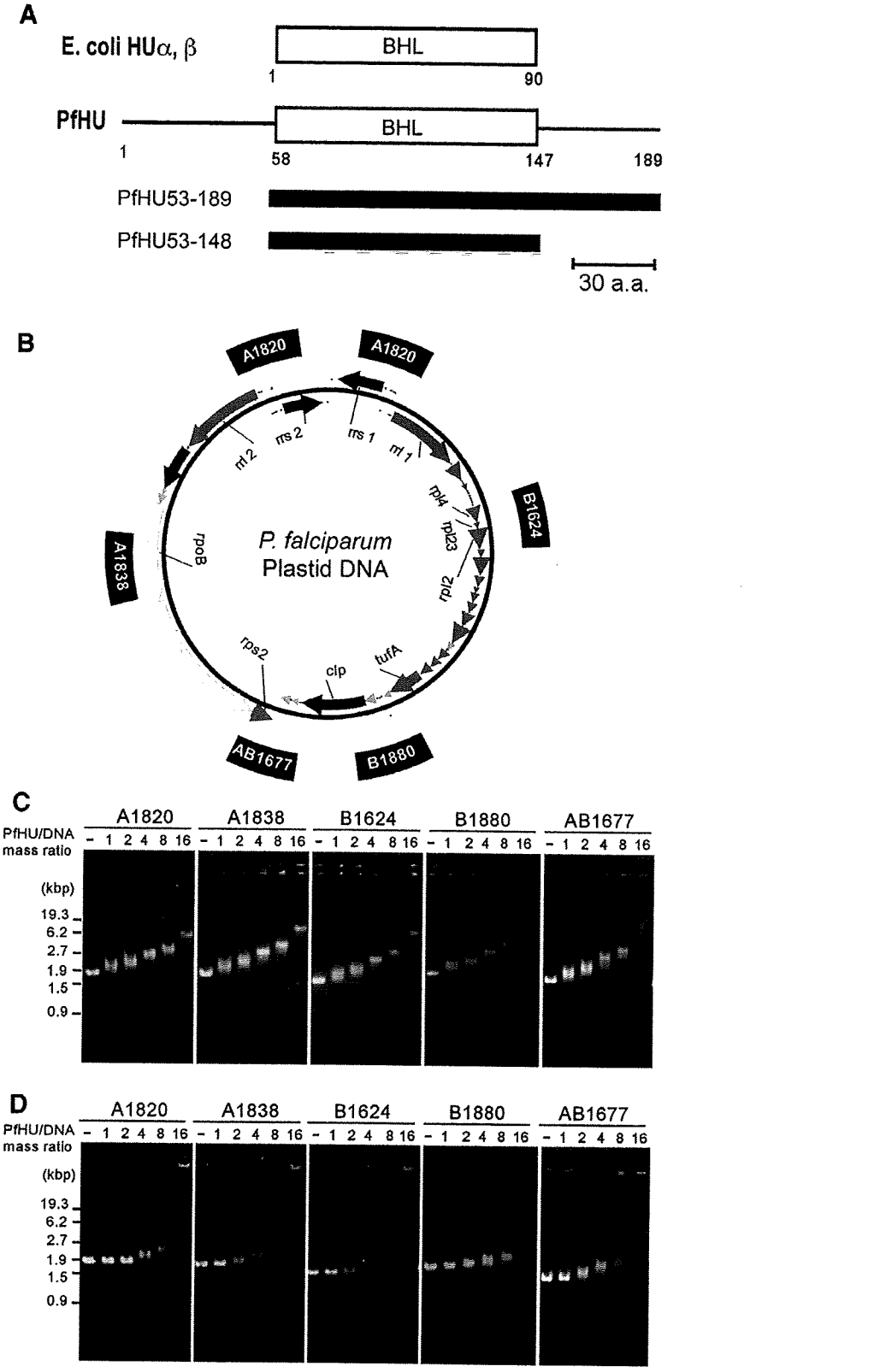

Fig. 1. PfHU binds the plastid DNA sequence-independently. (A) PfHU and its two recombinant forms. The BHL domain corresponding to the *E. coli* HU subunits is boxed. (B) Map of the plastid DNA of *P. falciparum*. The position of each DNA fragment used in the DNA-mobility shift assay is indicated outside the map. (C and D) DNA mobility shift assay. C, PfHU53-189; D, PfHU53-148. Note that the mobility of all fragments tested was similarly affected by each recombinant PfHU. The number of base pairs per one molecule of PfHU is 26 (PfHU53-189) or 18 (PfHU53-148), when the mass ratio of the protein to DNA is 1.